Global and site-specific characterization of the SUMO proteome by mass spectrometry

Hendriks, I.A.

Chapter 4

Site-Specific Identification of SUMO-2 Targets in Cells Reveals an Inverted SUMOylation Motif and a Hydrophobic Cluster SUMOylation Motif

Ivan Matic[1*], Joost Schimmel[2*], Ivo A. Hendriks[2*], Maria A. van Santen[2*], Frans van de Rijke[2], Hans van Dam[2], Florian Gnad[1], Matthias Mann[1], and Alfred C.O. Vertegaal[2]

[1]Department of Proteomics and Signal Transduction, Max-Planck Institute for Biochemistry, Martinsried D-82152, Germany
[2]Department of Molecular Cell Biology, Leiden University Medical Center, Leiden 2300 RC, The Netherlands
[*]These authors contributed equally to this work

Chapter 4 has been published in Molecular Cell

Mol Cell. 2010 Aug 27;39(4):641-52. doi: 10.1016/j.molcel.2010.07.026.
Supplementary Tables are available online.

ABSTRACT

Reversible protein modification by Small Ubiquitin-like Modifiers (SUMOs) is critical for eukaryotic life. Mass spectrometry-based proteomics has proven effective at identifying hundreds of potential SUMO target proteins. However, direct identification of SUMO acceptor lysines in complex samples by mass spectrometry is still very challenging. We have developed a generic method for the identification of SUMO acceptor lysines in target proteins. We have identified 103 SUMO-2 acceptor lysines in endogenous target proteins. 76 of these acceptor lysines are situated in the SUMOylation consensus site [VILMFPC]KxE. Interestingly, eight sites fit the inverted SUMOylation consensus motif [ED]xK[VILFP]. In addition, we found direct mass spectrometric evidence for crosstalk between SUMOylation and phosphorylation with a preferred spacer between the SUMOylated lysine and the phosphorylated serine of four residues. In 16 proteins we identified a Hydrophobic Cluster SUMOylation Motif (HCSM). SUMO conjugation of RanGAP1 and ZBTB1 via HCSMs is remarkably efficient.

INTRODUCTION

Ubiquitin (Ub) and ubiquitin-like proteins (Ubls) are covalently attached to other proteins via an isopeptide bond, which links the C-terminal glycine in these protein modifiers to the ε-amino group of lysines in substrate proteins. The Ubl family includes Nedd8, SUMO-1, -2, -3, ISG15, FAT10, FUBI, UBL5, URM1, ATG8 and ATG12. Reversible attachment of ubiquitin and Ubls to target proteins involves a set of enzymes [1-3]. Components of the SUMO system play critical roles in regulation of fundamental cellular processes such as gene expression, cell cycle progression, DNA replication and DNA repair [1, 4].

A significant number of previously identified SUMOylated lysines in target proteins reside within the consensus motif ΨKXE/D, where Ψ is a large hydrophobic amino acid and X is any amino acid. However, this motif also frequently occurs in non-SUMOylated proteins and many functionally important SUMO sites are known to be in non-consensus sequences. Therefore, bioinformatic analysis is not sufficient. Instead, SUMO sites need to be determined directly.

Mass spectrometry (MS)-based proteomics has established itself as the leading high-throughput proteomics technology and has become sufficiently mature to allow large scale studies of sub-proteomes and even entire proteomes [5, 6]. One of the main applications of MS is the direct mapping and quantitation of post-translational modifications (PTMs) of proteins. These modifications result in mass changes that can be detected by MS analysis [7]. Although all PTMs can potentially be studied by MS, site-directed large scale proteomics analysis of a specific PTM requires efficient enrichment of modified peptides. For example, for phosphorylation it is possible to identify thousands of modification sites [8, 9].

MS is also well suited for the characterization of Ub/Ubls substrate proteomes. However, in contrast to phosphorylation, the application of MS to the Ub/Ubl field currently relies on purification at the protein level. In a typical Ub/Ubl proteomics experiment for the study of these PTMs, targets covalently attached to the Ub/Ubl of interest are purified from cells expressing a tagged form of the modifier, such as His6-Ub or TAP-SUMO-2. Although this approach has been successfully employed to identify and quantify proteins modified by Ub/Ubls [10] [11-16], purification of intact modified species produces a peptide mixture that is too complex for efficient detection of Ub/Ubls modification sites. This is particularly problematic for SUMOylation since most SUMO substrates are low-abundant proteins and are modified at a small percentage.

In addition, the analysis of crosslinked peptides containing the large C-terminal SUMO sequence makes MS analysis challenging. Trypsin-digested SUMOs release large signature tags, such as 19 and 32 amino acids respectively for mammalian SUMO-1 and SUMO-2/3, which produce many fragment ions during MS/MS fragmentation. Although this makes the SUMO-crosslinked peptide identification unambiguous as compared to ubiquitin, it also makes identification

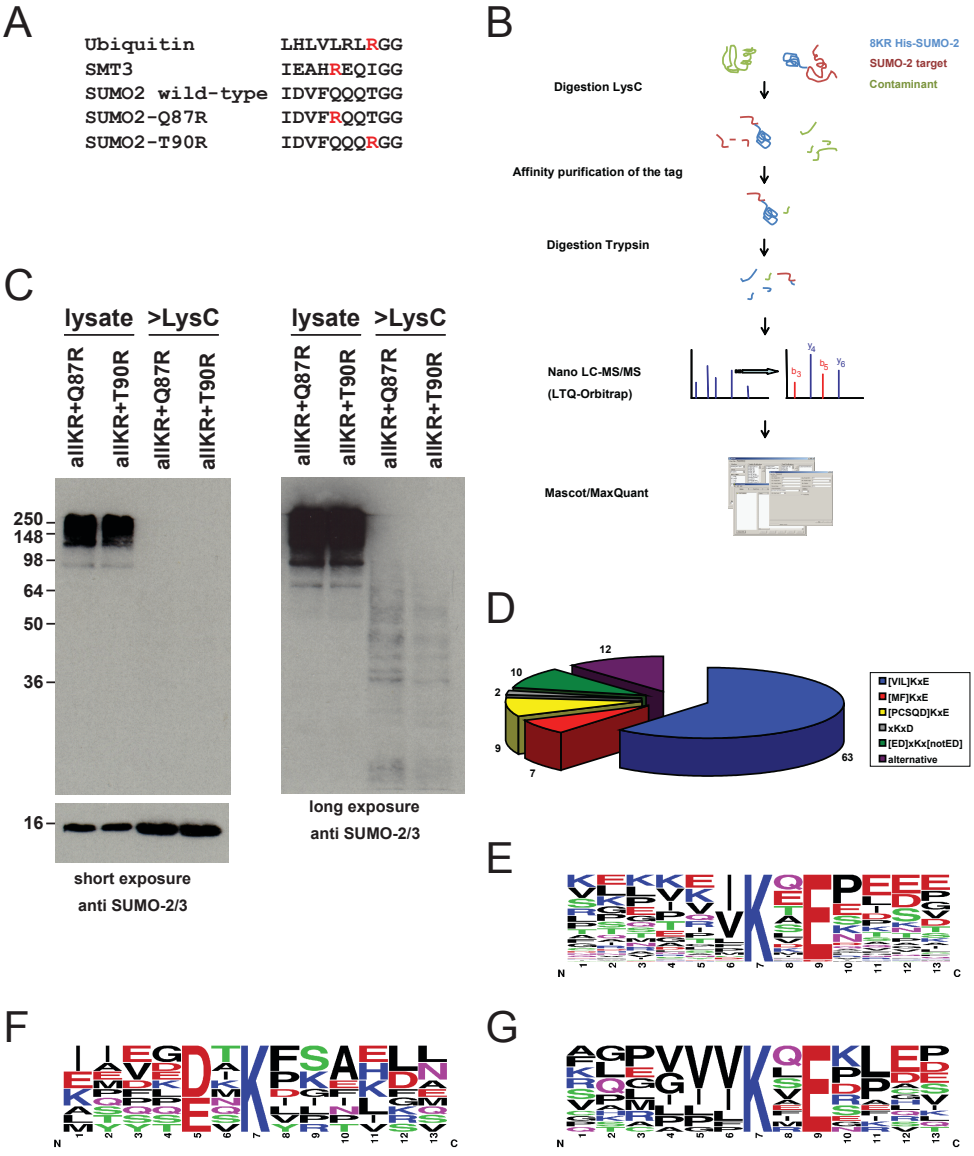

Figure 1. A method to identify SUMO acceptor lysines in endogenous target proteins purified from cell lysates.

A) The carboxyl-termini of mature ubiquitin, SMT3 and human SUMO-2 are depicted. Two SUMO-2 mutants were created, Q87R and T90R that contained arginines on positions corresponding to arginines in SMT3 or ubiquitin, respectively.

B) Purification Strategy. Lysine deficient His6-SUMO-2 mutants were expressed in HeLa cells and proteins in cell lysates were digested with endoprotease Lys-C that cleaves after lysine residues. His6-SUMO-2 and conjugated target protein fragments were purified by Immobilized Metal Affinity Chromatograpy (IMAC), digested with trypsin and analyzed by nano LC-MS/MS. Mascot and MaxQuant software were employed to identify SUMO-2 acceptor lysines in target proteins.

C) The SUMO-2 mutant proteins were efficiently conjugated to target proteins and conjugates were

challenging because the long modifying tryptic SUMO peptide leads to complex MS/MS fragmentation patterns. Several different approaches have been proposed for the identification of SUMOylated peptides. SUMmOn [17], a pattern recognition tool, in combination with low resolution mass spectrometry, has been successful in detecting peptides modified by SUMO *in vitro*. In a previous study we have applied a targeted mass spectrometric approach combined with the linearization of the branched peptides to detect SUMO polymerization sites *in vivo* [18]. In another approach, a database containing "linearized branched" peptides is employed to detect SUMO modified lysines [19]. Despite the validity and sophistication of these strategies, their application to *in vivo* samples has been limited by the much higher complexity of the peptide mixture and very low abundance of SUMO conjugates [20]. Here we report a method for selective enrichment of SUMOylated peptides from complex cellular proteomes. We have used this method to map SUMO modification sites in endogenous target proteins purified from cell lysates to obtain insight into protein SUMOylation.

RESULTS

A strategy to enrich SUMO modified peptides

In contrast to phosphorylation, direct identification of SUMO acceptor lysines in target proteins purified from cell lysates has remained very challenging. To selectively enrich SUMO modified peptides from cells, we employed a previously published His6-tagged SUMO-2 mutant in which internal lysines were replaced by arginines [13]. In addition, arginines were introduced at positions 90 (mutant T90R) or 87 (mutant Q87R; **Figure 1A**) to shorten the SUMO branched peptide generated after tryptic digestion [21]. The positions of these arginines correspond to the arginines that are present in ubiquitin or Smt3, respectively. Smt3 is the single SUMO family member found in *S. cerevisiae*. These mutants behave very similar to the wild-type counterpart (**Figure 2 and S2**) and related mutants have already been used successfully [22-24]. These lysine-deficient SUMO mutants are sensitive to digestion by trypsin, but not by Lys-C, an enzyme that specifically cleaves after lysine residues. After Lys-C digestion, peptides from target proteins that are covalently attached to lysine-deficient SUMOs via their SUMOylated lysines were

efficiently digested by Lys-C. Protein samples were analyzed by immunoblotting using an antibody directed against SUMO-2/3.

D) Out of the 103 SUMO-2 conjugated lysines that were detected in our screen 63 were situated in the SUMOylation consensus motif [VIL]KxE. Seven sites were situated in the consensus site [MF]KxE and nine were situated in [PCSQD]KxE sites. Ten SUMOylated lysines were situtated in the inverted consensus site [ED]xKx[≠ED] and two contained aspartic acids at position +2. Twelve SUMOylated lysines were missing acidic residues at position +2 or -2.

E-G) Graphical representations of the local target protein contexts of SUMO-2 conjugated lysines situated in the consensus motif KxE/D (E), in the inverted consensus motif E/DxKx[≠ED] (F) and in the Hydrophobic Cluster SUMOylation Motif (G). See also Figure S1.

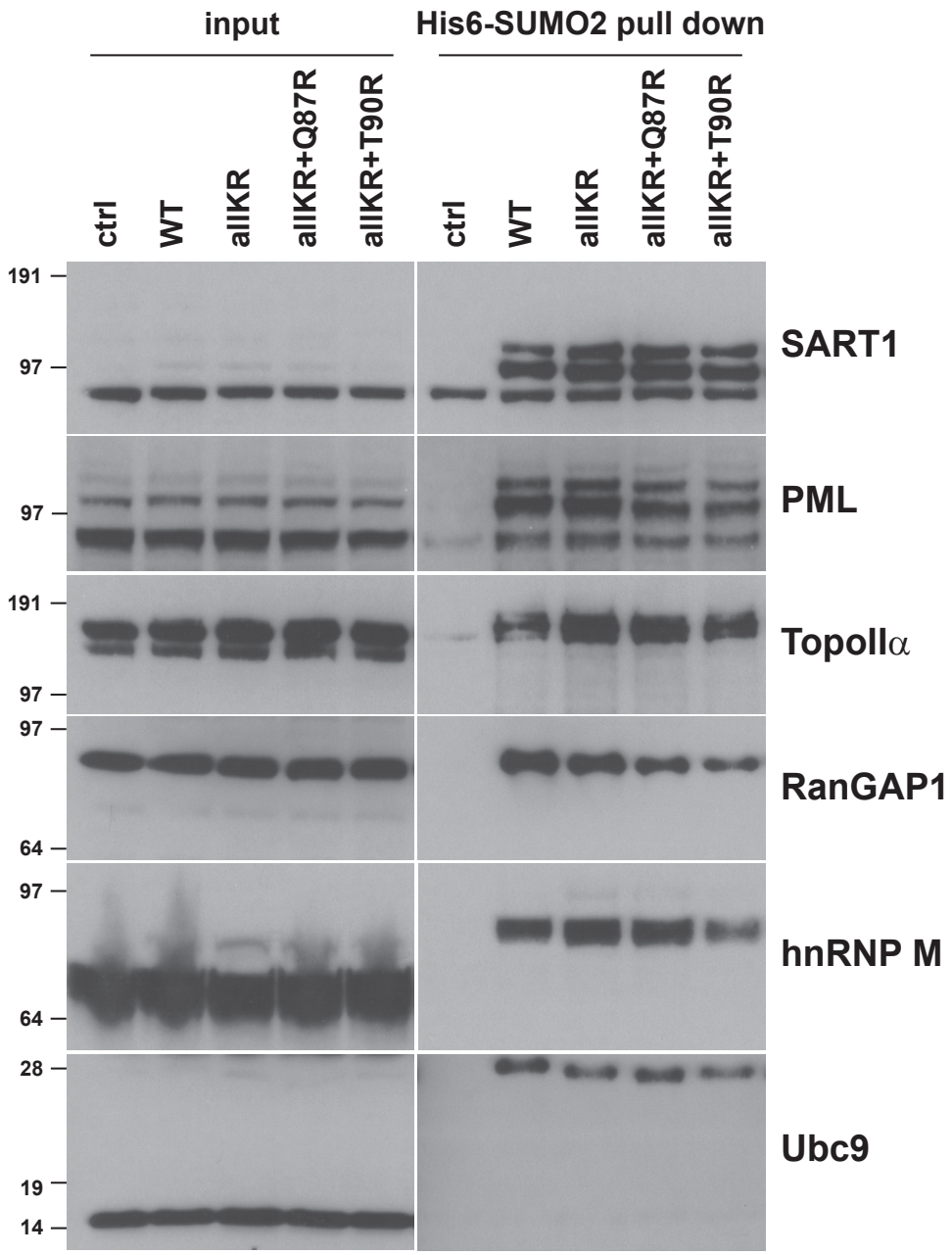

Figure 2. Verification of SUMO-2 mutants that were used for proteomics experiments.
HeLa cells were transfected with plasmids expressing wild-type His6-SUMO-2 or the indicated lysine-deficient His6-SUMO-2 mutants. Cells were lysed and SUMOs were purified by IMAC. Input and SUMO-2 enriched fractions were size-separated by SDS-PAGE, blotted onto membranes and probed with antibodies directed against SART1, PML, DNA Topoisomerase IIα, RanGAP1, hnRNP M or Ubc9. SUMO-2/3 probed immunoblots are depicted in Figure S2.

purified under denaturing conditions via the His6-Tag. Next, in solution or in gel tryptic digestion removed a large part of SUMO from the substrate peptides while leaving short SUMO remnants – namely GG for the T90R mutant and QQTGG in case of the Q87R mutant (**Figure 1B**). This is an efficient way to limit the complexity of the purified sample (**Figure 1C**).

Mass spectrometric mapping of SUMOylation sites

SUMOylated peptides were analyzed by nanoscale liquid chromatography coupled to high resolution hybrid mass spectrometers (LTQ-Orbitrap XL and LTQ-Orbitrap Velos) (see Materials and Methods). The LTQ Orbitrap Velos was operated in the higher-energy C-trap dissociation (HCD) mode, in which fragment ions are acquired with high resolution [25, 26]. Samples were analyzed multiple times using different acquisition strategies. SUMOylated peptides identified by standard database search were manually validated to maximize the confidence of identification (see Supplementary Material and Methods for a description of the measurements and for manual validation criteria). This was beneficial especially for the Q87R experiments because fragmentation of the QQTGG tag produced peaks that are not assigned by the search engine. During manual inspection of high resolution MS/MS spectra, we noticed the presence of QQTGG signature fragment ions in the low mass region, namely m/z 257.125 (QQ), m/z 240.097 (QQ with loss of ammonia) and m/z 239.114 (QQ with loss of water) (**Figure 3A and S1**). These ions were subsequently used as reporter ions for SUMOylated peptides.

Our strategy enabled the identification of 103 SUMOylated lysines from 82 endogenous target proteins (**Table S1**). This is significantly better than previous attempts [19, 22-24, 27]. Among the identified SUMOylated peptides, 69 were detected in both T90R and Q87R experiments, additionally validating the accuracy of our approach.

Analysis of SUMOylation Sites

Among the identified SUMO sites, 69% conformed to the previously established consensus site for SUMOylation, ΨKxE/D, were Ψ represents a large hydrophobic amino acid (**Figure 1D and E**). Remarkably, with the exception of the ΨKxD type site that we identified in H/ACA ribonucleoprotein complex subunit 2, all sites that fit the SUMOylation consensus contain a glutamic acid. SUMOylation of H/ACA ribonucleoprotein complex subunit 2 on lysine 5 was confirmed in the accompanying paper by Westman et al. The SUMOylated lysines were most frequently preceded by isoleucine, valine or leucine. Alternative amino acids that preceded the SUMOylated lysines were phenylalinine (4x), proline (4x), methionine (3x), cysteine (2x), aspartic acid (1x), glutamine (1x) and serine (1x) (**Table S1**). The validity of our approach was confirmed by the identification of previously published SUMO attachment sites in e.g. RanGAP1, PML, DNA topoisomerase I, PARP1, Sp1, Sp3 and SUMO-2 (**Table S1**).

The identification of SUMO attachment sites that are not situated in the

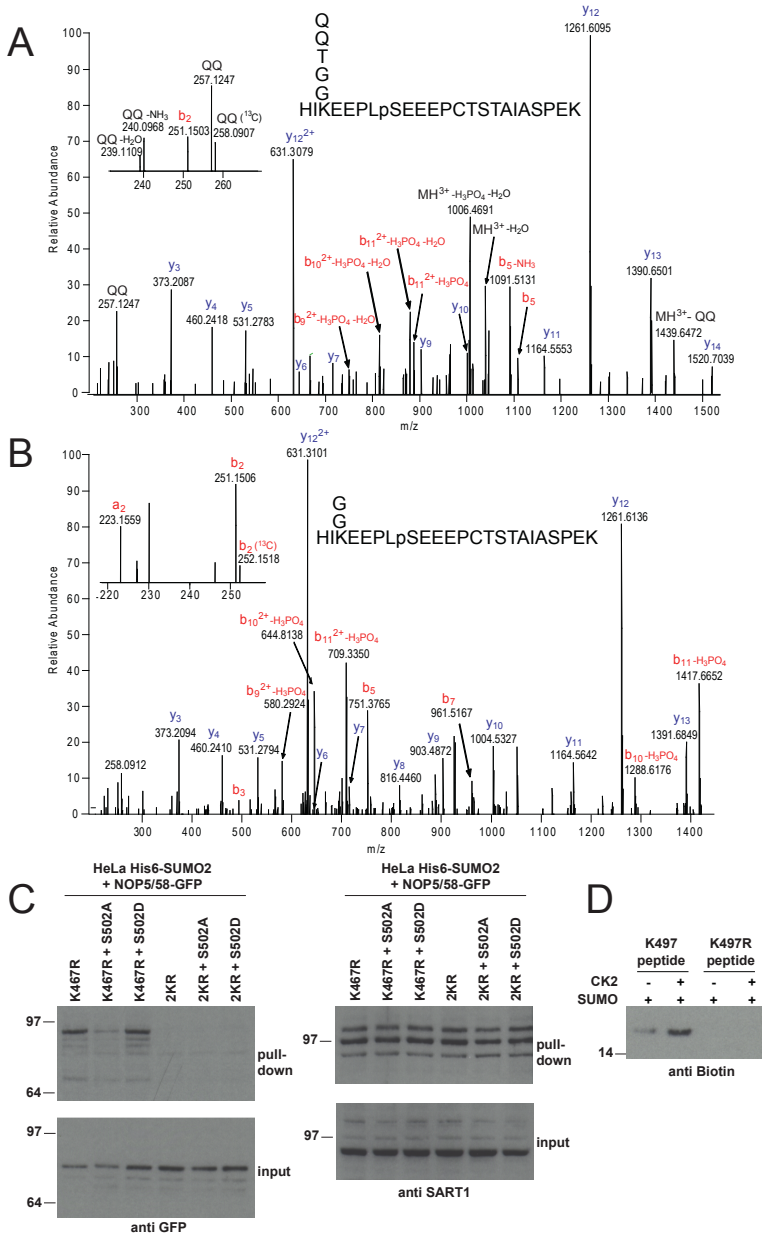

Figure 3. Phosphorylation-directed SUMOylation of NOP5/58.
A and B) Lysine 497 of NOP5/58 was identified as a SUMO-2 acceptor site in our screen using the SUMO-2 mutant Q87R (A) or the SUMO-2 mutant T90R (B). In both cases, the identified tryptic fragments contained phosphorylated serines on position 502. The doubly modified peptide was identified by high resolution tandem mass spectrometry using HCD fragmentation. Insets, magnifications of the low mass regions showing QQTGG signature fragment ions (A) and the a2/b2 pair (B). C) Serine 502 of NOP5/58 was mutated to alanine to prevent phosphorylation or to aspartic acid to mimick phosphorylation using a plasmid encoding NOP5/58-GFP. In addition, lysine 467 of NOP5/58 was mutated to arginine to avoid SUMOylation on this lysine residue. A double mutant (2KR) in

SUMOylation consensus motif remains a challenge. Interestingly, we identified ten SUMO attachment sites that contained acidic residues two positions upstream of the SUMOylated lysine (**Figure 1F and S1B**). The SUMOylated lysines were directly followed by phenylalanine (3x), proline (2x), isoleucine, leucine, valine, and also aspartic acid and tyrosine, so there is some preference for a hydrophobic residue. In contrast to the identified SUMO sites that matched the regular SUMOylation consensus motif, five of the inverted SUMOylation consensus sites contained an aspartic acid and the other five contained a glutamic acid at position -2. We have named this type of SUMOylation motif the inverted SUMOylation consensus motif E/DxKψ. Surprisingly, SUMO-1 contains an inverted SUMOylation consensus site that was empirically identified in the present study, indicating unexpected atypical chain formation between SUMO-2 and SUMO-1 [18, 28].

We were intrigued by the identification of SUMO attachment sites in ACIN1, ADAR, AHNAK, APC4, BRD4, FOSL2, GRL, hnRNP-M, NUMA1, RanGAP1, RSF1, SAFB2, SNIP-1, YLPM1, ZBTB1 and ZNF280C on lysines that were preceded by hydrophobic clusters of at least three hydrophobic residues instead of the single hydrophobic residue that is usually present (**Figure 1G and Table S1**). We have named this type of SUMOylation site the Hydrophobic Cluster SUMOylation Motif (HCSM). These results will help to predict SUMO attachment sites in proteins. To facilitate the prediction of SUMOylation sites in proteins based on our results, we created a SUMOylation motif matcher in the Phosida database (http://www.phosida.com) [29].

Interestingly, SUMO-acceptor lysines in BRD4 (K1111), RanGAP1 (K526), SAFB2 (K293) and Treacle protein TCOF1 (K755) (**Table S1**) were previously identified as acetylated lysines [18, 30]. Since SUMOylation and acetylation are mutually exclusive, this indicates competition between acetylation and SUMOylation for the same lysines.

Crosstalk between SUMOylation and phosphorylation

Our mass spectrometry results revealed that the SUMOylated tryptic peptides of NOP5/58, RBM25, APC4, SNIP-1 and TOP2 contained downstream phosphorylated serines (**Figure 3 and S3**). The spacing between the SUMOylated lysines and the downstream phosphorylated serines is remarkably consistent in NOP5/58, RBM25, SNIP-1 and APC4 with a preferred spacer of four amino acids between the SUMOy-

which lysines 467 and 497 were replaced for arginines was included as a negative control. HeLa cells expressing His6-SUMO-2 were transfected with these plasmids or with the wild-type control. Lysates were prepared and His6-SUMO-2 conjugates were purified by IMAC. Protein samples were analyzed by immunoblotting using antibodies against GFP and against SART1 as a control.

D) A biotin-tagged NOP5/58 PDSM peptide (residues 495-505 Biotin-HIKEEPLSEEE) and control peptide (Biotin-HIREEPLSEEE) were synthesized, phosphorylated in vitro by Casein Kinase 2 and SUMOylated. After termination of the reaction with LDS sample buffer, samples were size-separated by SDS-PAGE and immunoblots were analyzed using an antibody against the Biotin-tag. See also Figure S3.

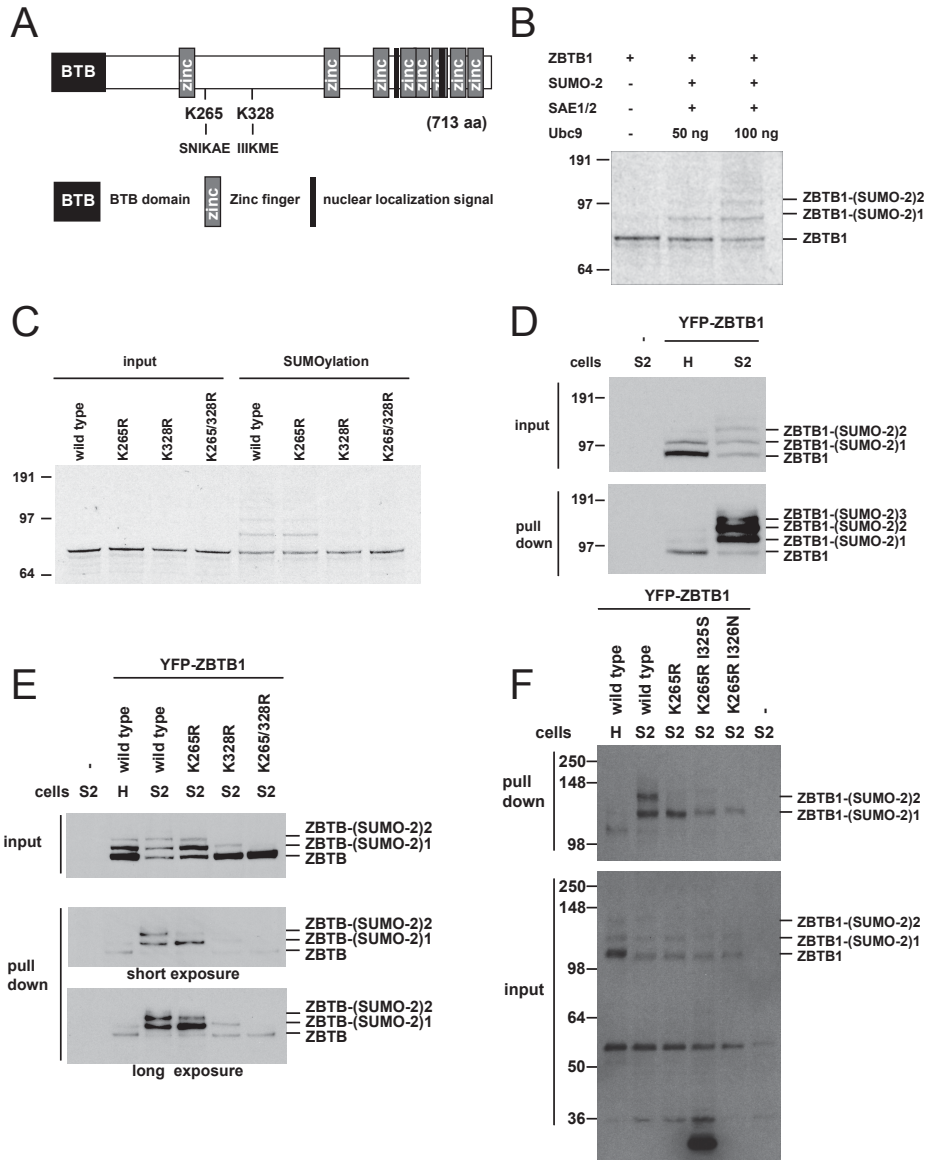

Figure 4. A Hydrophobic Cluster SUMOylation Motif mediates efficient conjugation of ZBTB1 to SUMO-2.

A) Cartoon depicting Zinc finger and BTB domain protein 1 (ZBTB1). ZBTB1 is composed of 713 amino acids and harbors a BTB domain, eight C_2H_2-type zinc fingers, two nuclear localization signals and two consensus SUMOylation sites (K265, K328).

B) ZBTB1 is SUMOylated *in vitro*. An *in vitro* SUMO-2 conjugation reaction was performed, containing SUMO-2, SAE1/2, and Ubc9 as indicated and *in vitro* transcribed and translated [^{35}S] labeled ZBTB1. The reaction was incubated for 3 hours at 37°C. After termination of the reaction by adding LDS sample buffer, samples were fractionated by SDS-PAGE, and dried gels were subjected to autoradiography.

C) The *in vitro* SUMOylation experiment was repeated including ZBTB1 mutants lacking one or two SUMOylation sites (K265R, K328R or double mutant).

lated lysine and the phosphorylated serine (**Table S1, Figure S3**). To establish the relevance of the phosphorylation of serine 502 in NOP5/58, we mutated this serine to alanine and studied the SUMOylation of this mutant (**Figure 3C**). Our results indicate that phosphorylation of NOP5/58 on serine 502 is a pre-requisite for the SUMO conjugation of lysine 497. Remarkably, the three glutamic acids on positions 503-505 were not able to compensate for the absence of the serine in the S502A mutant. Serine 502 is situated in the Casein Kinase II consensus phosphorylation site [ST]xx[ED]. Consistently, Casein Kinase II-mediated phosphorylation of a peptide matching the SUMO-phospho motif in NOP5/58 enhanced its SUMOylation (**Figure 3D**). Functionally, the SUMOylation of NOP5/58 is relevant for snoRNA binding (Westman et al. accompanying manuscript).

SUMOylation of ZBTB1 via an extended SUMOylation motif

The Hydrophobic Cluster SUMOylation Motif in ZBTB1 was studied in detail by mutagenesis (**Figure 4**). The ZBTB1 protein contains an amino-terminal BTB domain, eight Zinc fingers, two nuclear localization signals and two lysines situated in the SUMOylation consensus motif ΨKxE, lysines 265 and lysine 328 (**Figure 4A**). Lysine 328 was identified in our screen for SUMOylated lysines and is preceded by three consecutive isoleucines (**Figure S4A**). ZBTB1 was efficiently conjugated to SUMO-2 *in vitro* mainly via lysine 328 and to a lesser extent via lysine 265 (**Figure 4B and 4C**). Similar results were obtained for SUMOylation of ZBTB1 in cells, uncovering a remarkably efficient SUMOylation of this protein (**Figure 4D, 4E and S4B**). The hydrophobic cluster preceding lysine 328 enhanced the SUMOylation efficiency, since mutating the isoleucines to corresponding amino acids serine and asparagine that precede the less efficiently SUMOylated lysine 265 significantly reduced the SUMO conjugation of lysine 328 (**Figure 4F**). This strikingly efficient SUMOylation site does not consist of an integrated SUMO Interaction Motif (SIM) and a SUMOylation site, since mutating the isoleucines on position 325 and 326 to alanines did not affect the SUMOylation efficiency (**Figure S4C**) in contrast to SIM-mediated SUMO conjugation of USP25 [31].

D) ZBTB1 is SUMOylated *in vivo*. HeLa cells stably expressing His6-SUMO-2 (S2) and control HeLa (H) cells were transfected with an expression construct encoding YFP-ZBTB1. Cells were lysed 24 hours after transfection in 8M Urea and His6-SUMO-2 conjugates were purified by IMAC. Total lysates (inputs) and purified fractions (pull down) were separated by SDS-PAGE, transferred to a membrane and probed using an antibody to detect YFP.

E) The experiment described in D was repeated including ZBTB1 mutants lacking one or two SUMOylation sites (K265R, K328R or double mutant).

F) Hydrophobic residues on position 325 and 326 of ZBTB1 affect the efficiency of ZBTB1 SUMOylation. The experiments described in D and E were repeated including ZBTB1 K265R mutants that are only SUMOylated on lysine 328. Hydrophobic residues on positions 325 or 326 were replaced for the corresponding amino acids preceding lysine 265. See also Figure S4.

The BTB domain regulates the SUMOylation level of ZBTB1

Four ZBTB family members were identified in our SUMOylation site screen, ZBTB1, ZBTB2, ZBTB9 and ZBTB38. Previously, the BTB domain has been shown to mediate protein ubiquitination via interaction with Cul-3 [32]. Furthermore, the BTB-domain enables BTB-proteins to oligomerize. To test whether the BTB domain is involved in protein SUMOylation, we created a ZBTB1 mutant lacking the BTB domain (**Figure 5A and B**). As expected, this mutant lacked the capacity to form oligomers (**Figure 5C**). A striking decrease in SUMOylation was observed for the mutant protein compared to wild-type ZBTB1, indicating that an intact BTB domain is required for the efficient SUMOylation of ZBTB1 (**Figure 5D**). Subsequently, we tested whether the recombinant BTB domain can enhance SUMOylation in trans. GST-BTB(aa1-141) was produced in *E.coli*, purified and added to *in vitro* SUMOylation reactions (**Figure 5E**). Addition of recombinant BTB domain to these SUMOylation assays did not alter the SUMOylation efficiency of ZBTB1, indicating that the BTB domain functions in cis via oligomerization. Thus, the ZBTB1 oligomer is more efficiently SUMOylated compared to the monomer [33].

SUMOylation inhibits the repressive activity of ZBTB1

Some ZBTB family members act as transcriptional repressors (Deweindt et al., 1995; Numoto et al., 1993; Li et al., 1997; Koh et al., 2009; Jeon et al., 2009). Since the target genes of ZBTB1 are currently unknown, we employed the Gal4 system [34] to study the transcriptional activity of ZBTB1. The thyroid hormone receptor fused to the Gal4 DNA binding domain was used as a control repressor in this experiment. In the absence of hormone, this receptor repressed the Gal4 binding site containing luciferase reporter 6.1 fold whereas ZBTB1 repressed this reporter construct 10.6 fold, indicating that ZBTB1 is a potent transcriptional repressor (**Figure 6A**). In general, SUMOylation inhibits transcription factors [35]. Here, we show that SUMOylation of ZBTB1 via lysine 265 reduces its repressive activity (**Figure 6B, 6C, S5A and S5B**). The location of the SUMOylated lysine in the protein appears to be important since SUMOylation of lysine 328 did not affect the repressive activity of ZBTB1.

SUMOylation regulates subnuclear partitioning of ZBTB1

SUMOylation can affect the subcellular localization of proteins as demonstrated for RanGAP1, Sp3 and other proteins [36]. Confocal microscopy was used to study the subcellular localization of YFP-ZBTB1 (**Figure 6D**). This revealed that ZBTB1 is a nuclear protein, which was expected since the protein harbors two nuclear localization signals (aa574-578 and aa645-652) (Fig 4A). ZBTB1 mainly localized to the nucleoplasm and accumulated in nuclear bodies. These ZBTB1 nuclear bodies did not colocalize with PML (data not shown) in contrast to the BTB domain containing protein Bach2 [37] but did colocalize with the transcriptional repressor SMRT (**Figure 6E**). Next, we compared the subcellular localization of wild-type and

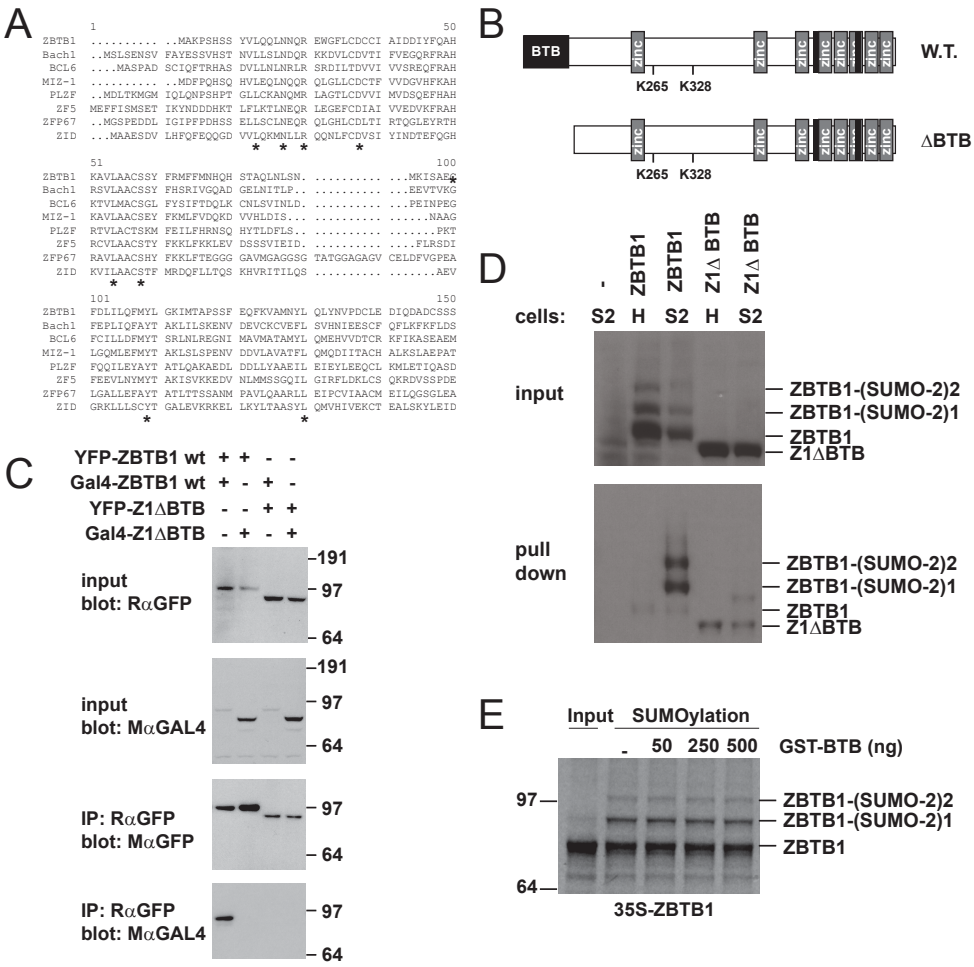

Figure 5. A role for the BTB domain in protein SUMOylation.

A) BTB domains of ZBTB1, Bach1, BCL6, MIZ-1, PLZF, ZV5, ZFP67 and ZID were aligned.

B) A ZBTB1 deletion construct was created that lacked the BTB domain. This ΔBTB mutant lacked the first 142 amino acids of the wild-type ZBTB1 protein.

C) Wild-type ZBTB1 and the ΔBTB mutant were fused to YFP or Gal4. These proteins were transiently expressed in HeLa cells and immunoprecipated from lysates using rabbit anti GFP antibody. Inputs and immunoprecipitates were analyzed by immunoblotting using mouse anti GFP antibody and mouse anti Gal4 antibody.

D) HeLa cells stably expressing His6-SUMO-2 (S2) and control HeLa (H) cells were transfected with expression construct encoding YFP-ZBTB1 wild-type or ΔBTB mutant. His6-SUMO-2 conjugates were purified from a denaturing lysate and analyzed by immunoblotting to visualize SUMOylated ZBTB1.

E) Recombinant GST-BTB domain (aa1-141) was generated in *E. coli* and added to *in vitro* SUMOylation assays using [^{35}S] labeled ZBTB1 as a substrate. The reaction was incubated for 3 hours at 37^{o}C. After termination of the reaction by adding LDS sample buffer, samples were fractionated by SDS-PAGE, and dried gels were subjected to autoradiography.

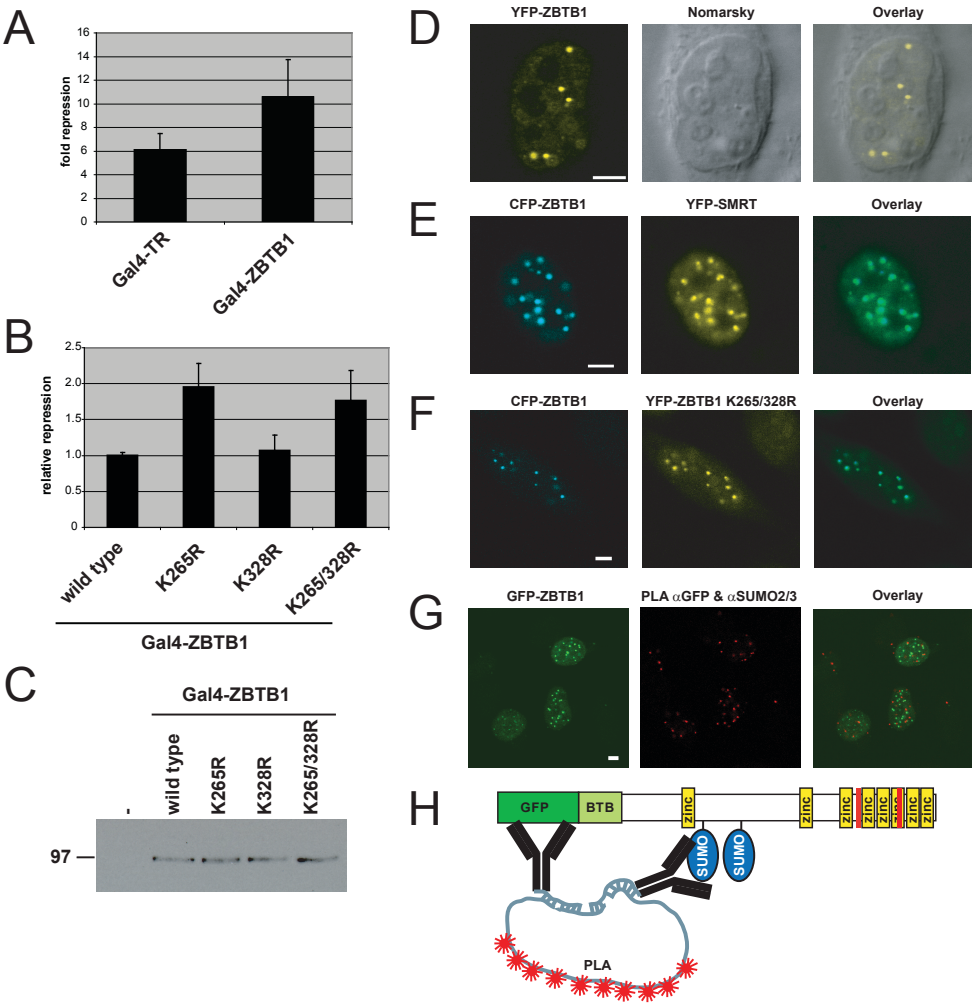

Figure 6. SUMOylation regulates the transcriptional activity and subcellular localization of ZBTB1.
A-C) HeLa cells were grown on 24-well dishes and transfected with 500 ng of Gal4(DBD)-fusion expression plasmids and 500 ng of the reporter construct 5xGal4-Tk-Pgl3. Cells were lysed in reporter lysis buffer 24 hours after transfection and luciferase activity was measured. Results are representative of four independent experiments; the error bars indicate one standard deviation from the average.
A) The transcriptional activity of Gal4-ZBTB1 was compared to the known transcriptional repressor thyroid hormone receptor (TR) fused to Gal4.
B) The transcriptional activities of Gal4-ZBTB1 wild type and SUMOylation mutants were determined.
C) Transfection mixtures were split and one set of wells was lysed in LDS sample buffer to verify the expression levels of the Gal4-ZBTB1 proteins by immunoblotting using an antibody directed against Gal4.

SUMOylation-deficient ZBTB1 (**Figure 6F**). Both proteins colocalize in the nucleoplasm and in nuclear bodies. SUMOylation-deficient ZBTB1 can still interact with wild-type ZBTB1 via BTB-domain mediated oligomerization, therefore, this experiment does not reveal the specific subcellular localization of the SUMOylated form of ZBTB1. To positively identify the location of SUMOylated ZBTB1, we adapted the Proximal Ligation Assay (PLA) [38, 39] for protein SUMOylation. The PLA principle is depicted in the cartoon in **Figure 6H**. Primary antibodies directed against GFP and SUMO-2/3 and secondary antibodies labeled with oligonucleotides were employed to reveal the location of SUMOylated ZBTB1 (**Figure 6G**). The GFP signal represents the location of SUMOylated and non-SUMOylated ZBTB1. PLA signals were located in the nucleoplasm, but not in the nuclear bodies, indicating that SUMOylated ZBTB1 is located in the nucleoplasm outside the nuclear bodies. No detectable PLA signal was observed for the SUMOylation-deficient ZBTB1 mutant (**Figure S5C**). We conclude that SUMOylation regulates ZBTB1 via altering its subcellular localization.

Efficient conjugation of RanGAP1 to SUMO is mediated by a HCSM

RanGAP1 was the first identified SUMO substrate and is very efficiently conjugated to SUMO via lysine 526 [40, 41] that is situated in the Hydrophobic Cluster SUMOylation Motif GLLKSE. To verify whether this HCSM is involved in RanGAP1 SUMOylation, we deleted glycine 523 and leucine 524, or replaced these residues for the basic residue histidine or the polar residue asparagine. SUMOylation of these mutants was severely reduced compared to wild-type RanGAP1 indicating that glycine 523 and leucine 524 contribute to the efficient SUMOylation of RanGAP1 (**Figure 7A**). Consistently, RanGAP1 HCSM mutants failed to accumulate at nuclear pore complexes due to reduced SUMOylation (**Figure 7B**) [40, 41].

D-H) HeLa cells were (co)transfected with expression constructs encoding YFP-ZBTB1, CFP-ZBTB1, GFP-ZBTB1, YFP-ZBTB1 K265/328R or YFP-SMRT. Cells were fixed and analyzed by confocal microscopy. Scale bars are 4 μm.

D) YFP-ZBTB1 localizes to the nucleoplasm and accumulates in nuclear bodies.

E) Colocalization of CFP-ZBTB1 and YFP-SMRT.

F) Colocalization of CFP-ZBTB1 and YFP-ZBTB1 K265/328R.

G) Proximal Ligation Assay (PLA) to detect SUMOylated ZBTB1. Cells were transfected with an expression construct encoding GFP-ZBTB1, fixed and the PLA was performed using affinity purified peptide anti SUMO-2/3 antibodies and a monoclonal antibody directed against GFP. Secondary antibodies were labeled with specific oligonucleotides. Oligonucleotide hybridization, ligation, amplification and detection were performed.

H) The cartoon briefly depicts the PLA technique. See also Figure S5.

DISCUSSION

Reversible post-translational modification of proteins by small chemical groups and small proteins enables tight control of protein activity. Recently, global analysis of protein phosphorylation dynamics by mass-spectrometry has enabled system-wide insight into signal transduction networks [30, 42, 43]. Mass-spectrometric analysis of protein SUMOylation is currently very challenging [16]. We have developed a MS-based method to map acceptor lysines for SUMOs in endogenous substrate proteins purified from cells. The majority of the identified SUMO acceptor lysines were situated in the SUMOylation consensus motif ψKxE. In addition, we have uncovered an inverted SUMOylation consensus motif E/DxKψ and an extended SUMOylation consensus motif, the HCSM, where the SUMOylated lysine is preceded by a cluster of at least three hydrophobic amino acids. Moreover, we uncovered crosstalk between SUMOylation and phosphorylation and competition between SUMOylation and acetylation.

Most SUMO acceptor lysines are currently identified using site-directed mutagenesis of potential SUMO acceptor sites. This method is very laborious and is unable to discriminate between SUMOylation sites and sites whose mutation changes the substrates and results in loss of SUMOylation at distal lysines [16]. In studies on SUMOylation in yeast by the Gygi laboratory, six SUMOylation sites were identified [27] and in a study by the Yates laboratory, 22 sites were identified using the Smt3 I96R mutant and seven sites using wild-type Smt3 [23]. In the most comprehensive study on protein SUMOylation in mammalian cells [44], five SUMOylation sites were identified. Recently, 14 SUMOylation sites were identified by Blomster et al. (2010) and a single SUMO site was identified by “ChopNspice” in endogenous proteins purified directly from cells and 17 sites including 8 sites on the SUMO E3 ligase RanBP2 by “ChopNspice” after incubation of a cellular extract with ATP [19]. Our methodology enabled us to identify significantly more SUMOylation sites in endogenous target proteins purified directly from cells and yielded important insight into SUMOylation motifs.

The identification of SUMO attachment sites in target proteins that lack classical SUMOylation consensus sites is very challenging and this has hampered progress in the field. The discovery of the inverted SUMOylation consensus sites E/DxKΨ in our study could be particularly useful to predict SUMOylation sites in these target proteins and enable direct follow up by mutagenesis of SUMO targets that contain these motifs.

The SUMO-phospho modified sites that we identified in our screen in NOP5/58, RBM25, APC4, SNIP-1 and TOP2 did not strictly fit the previously published Phosphorylation-Dependent SUMOylation Motif (PDSM) ΨKxE/DxxSP since the phosphorylation event was only proline-directed in SNIP-1 [45]. This indicates more extensive crosstalk between phosphorylation and SUMOylation than previously anticipated. Interestingly, it has recently been shown that phosphorylation of the

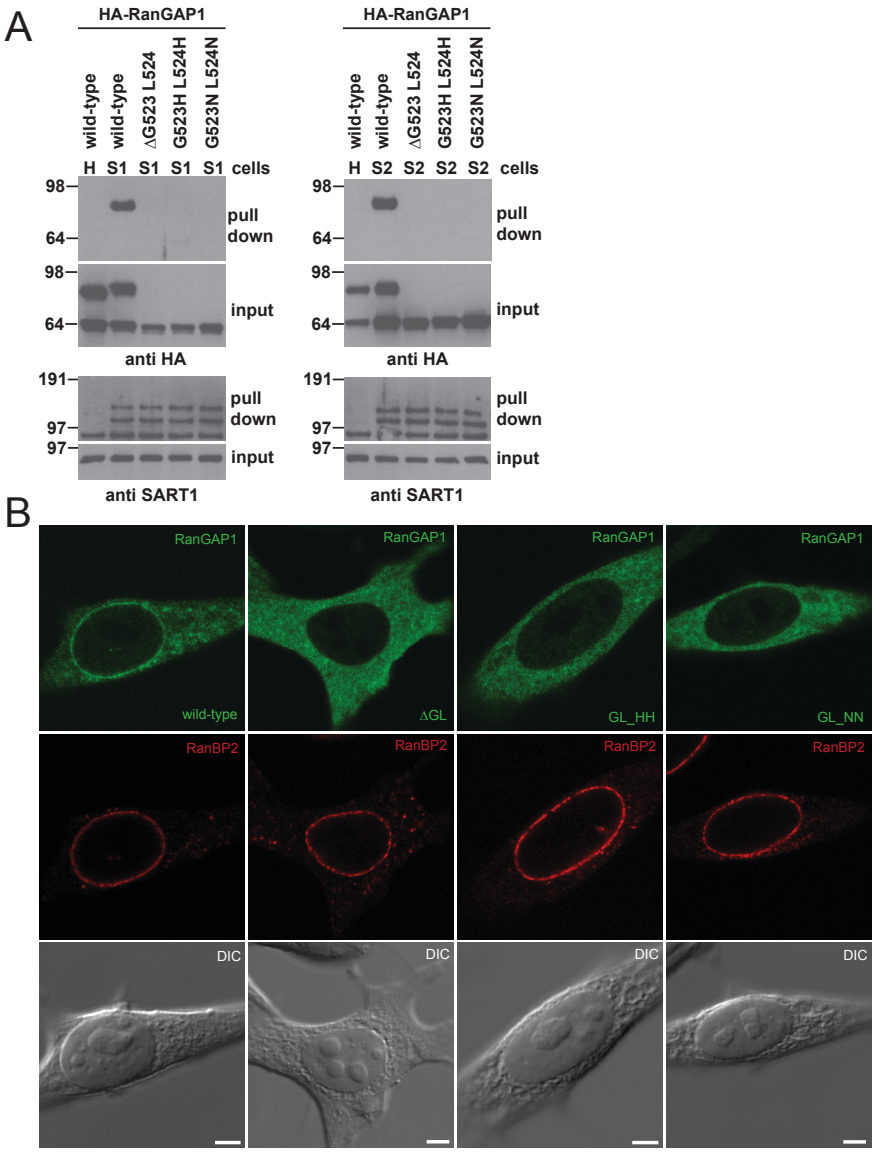

Figure 7. A Hydrophobic Cluster SUMOylation Motif mediates efficient conjugation of RanGAP1 to SUMO.

A) HeLa cells stably expressing His6-SUMO-1 (S1) or His6-SUMO-2 (S2) and control HeLa (H) cells were transfected with expression constructs encoding HA-RanGAP1 wild-type or the indicated HCSM mutants. Cells were lysed 24 hours after transfection and His6-SUMO conjugates were purified by IMAC. Total lysates (inputs) and SUMO purified fractions (pull down) were separated by SDS-PAGE, transferred to membranes and probed using antibodies against HA and against SART1 as a control.

B) HeLa cells were transfected with expression constructs encoding HA-RanGAP1 wild-type or the indicated HCSM mutants. Cells were fixed, co-stained with antibodies against the HA-tag (green) and against the nucleoporin RanBP2 (red) and analyzed by confocal microscopy. Scale bars are 4 μm.

PDSM motif in Myocyte Enhancement Factor 2 and Heat-shock Transcription Factor 1 mediates the binding of this protein to a basic patch in the SUMO E2 ligase Ubc9, providing mechanistic insight into crosstalk between SUMOylation and phosphorylation [18, 46].

Phosphorylated residues downstream of SUMOylation sites that enhance protein SUMOylation can functionally be replaced by negatively charged residues in the Negatively charged amino acid-Dependent SUMOylation Motif (NDSM) [47]. Consistently, we found that the most frequently occurring amino acids five positions downstream of the SUMOylated lysines are glutamic acid, aspartic acid and serine. Positively charged residues were frequently found upstream of SUMOylated lysines and can enhance SUMOylation efficiency [48].

We have identified an additional type of extended SUMOylation motif in our screen, the Hydrophobic Cluster SUMOylation Motif (HCSM). Mutagenesis experiments with the HCSMs in ZBTB1 and RanGAP1 indicated that these sites are very efficiently used for SUMO conjugation possibly due to enhanced binding to the SUMO E2 enzyme Ubc9 [49]. Unexpectedly, the BTB domain was required for the efficient SUMOylation of ZBTB1. Previously, the BTB-domain was shown to function in protein ubiquitination as an adapter protein for Cul-3 [32, 50]. Mechanistically, the BTB domain mediates oligomerization, therefore, we expect that the ZBTB1 oligomer is more efficiently SUMOylated due to Ubc9 hopping to the different moieties of the oligomer. SUMOylated ZBTB1 does no longer co-localize with the co-repressor SMRT in nuclear bodies, thus we expect that SUMOylation regulates ZBTB1 activity via altering its subcellular localization.

We present a strategy for selective enrichment of SUMO modified peptides in complex cellular proteomes. The identified SUMOylated lysines and the discovery of SUMOylation motifs will provide a useful resource for the increasingly important SUMO field.

EXPERIMENTAL PROCEDURES

Plasmids

Plasmid constructs are described in Supplemental Experimental Procedures.

Cell lines, cell culture and transfection

HeLa cells and HeLa cells stably expressing His6-SUMO-2 ($HeLa^{His6SUMO-2}$) [14] were cultured in Dulbecco's modified Eagle's medium (DMEM) (Invitrogen), supplemented with 10% FCS and 100 U/ml penicillin and streptomycin (Invitrogen). Transfections were carried out using 2.5 μl Polyethylenimine (PEI, 1 mg/ml, Alpha Aesar) per μg DNA or using Lipofectamine 2000 (Invitrogen) according to the instructions of the manufacturer.

Antibodies

Peptide antibody AV-SM23-0100 (Eurogentec) against SUMO-2/3 and peptide antibody 1607 against SART1 were described previously [14, 15]. Monoclonal antibody 5E10 against PML was a kind gift from Dr. Van Driel (Amsterdam, the Netherlands) and goat antibody against RanBP2 was a kind gift from Dr. Melchior (Heidelberg, Germany). Other antibodies that we used were mouse anti-HA, mouse anti-GFP (Roche), rabbit anti GFP (Invitrogen) mouse anti-Gal4 (Santa-Cruz Biotechnology), mouse anti Ubc9

and mouse anti DNA Topoisomerase IIα (BD Biosciences), mouse anti RanGAP1 (Zymed) and mouse anti hnRNP M (Sigma).

Purification of SUMOylated proteins for mass spectrometry

Transfected cells were harvested in icecold PBS. Cells were lysed in 6M Guanidinium-HCl containing 0.1M $NaHPO_4$ and 0.01M Tris/HCl pH8.0. Samples were filtered 3 times over Qiashredders (Qiagen) to reduce the viscosity. After centrifugation for 5 minutes at 14K, proteins in the supernatants were reduced using 1 mM dithiothreitol and alkylated using 5 mM iodoacetamide at room temperature. Proteins were digested by endoprotease Lys-C and His6-SUMO-2 conjugates were purified using Ni^{2+}-NTA agarose beads. Beads were washed twice with lysis buffer and 5 times with 8M Urea containing 0.1M $NaHPO_4$ and 0.01M Tris/HCl pH 8.0. Samples were eluted in 6.4 M Urea pH 8.0 containing 200 mM imidazole. The eluted His6-SUMO-2 conjugates were diluted 4 times with 10 mM ammonium bicarbonate and digested in solution with trypsin for 12 hours at room temperature. In a separate set of experiments, the His6-SUMO-2 conjugates were separated by SDS-PAGE and the bands in the molecular weight range 15-38 kDa were excised from the gel and subjected to in-gel digestion [51].

Mass spectrometric analysis

The procedure is detailed in supplementary materials and methods. Briefly, the trypsin-digested peptides were purified on StageTips [52] and analyzed by nanoscale LC-MS/MS on a LTQ-Orbitrap XL or LTQ-Orbitrap Velos mass analyzer (Thermo Fisher Scientific, Germany) coupled to EASY-nLC system (Proxeon Biosystems, Denmark). Raw MS data were processed with MaxQuant [53, 54] and the Mascot search engine (Matrix Science, UK). MS/MS spectra of identified SUMO modified peptides were manually validated and are available upon request. The identified sites were aligned using WebLogo (Computational Genomics Research Group, University of California, Berkeley).

Microscopy and Proximity Ligation Assay

Cells were grown on glass coverslips and transfected with expression constructs encoding EGFP-, EYFP- ECFP- or HA-tagged proteins. Cells were fixed 24 hours after transfection for 10 minutes in 3.7% paraformaldehyde in PHEM buffer (60 mM PIPES, 25 mM HEPES, 10 mM EGTA, 2 mM MgCl2, pH 6.9) at 37°C. After washing with PBS, cells were mounted in Vectashield (Vector Laboratories). Immunostaining was performed as previously described (Matunis et al., 1998). Secondary antibodies were rabbit anti goat Alexa 594 and rabbit anti mouse Alexa 488 (Invitrogen). Proximity Ligation was performed as previously described [38, 39]. Images were recorded on a Leica TCS/SP2 confocal microscope system using a 100x NA 1.4PL APO lens and were analyzed with Leica confocal software.

ACKNOWLEDGMENTS

This work was supported by the Netherlands Organisation for Scientific Research (NWO) (to A.C.O.V.) and the RUBICON EU Network of Excellence (to M.M.) I.M. is the recipient of a fellowship from RUBICON. We would like to thank Drs. A.I. Lamond and B. Westman for sharing unpublished data and reagents. We would like to thank Drs. F. Melchior, C. Lima, S. Zanivan and E. Meulmeester for helpful discussions. We are grateful to Drs. F. Melchior, G. Gill, N. Perkins, R. van Driel, M. Posch, E. Kalkhoven, E.J. Park and J.D. Chen for providing critical reagents and to Dr. M. Tatham for comparisons with previously published SUMO target proteomes.

Reference List

1. Geiss-Friedlander, R., and Melchior, F. (2007) Concepts in sumoylation: a decade on. *Nat. Rev. Mol. Cell Biol.* 8, 947-956
2. Hay, R. T. (2007) SUMO-specific proteases: a twist in the tail. *Trends Cell Biol.* 17, 370-376
3. Mukhopadhyay, D., and Dasso, M. (2007) Modification in reverse: the SUMO proteases. *Trends Biochem. Sci.* 32, 286-295
4. Bergink, S., and Jentsch, S. (2009) Principles of ubiquitin and SUMO modifications in DNA repair. *Nature* 458, 461-467
5. Cox, J., and Mann, M. (2007) Is proteomics the new genomics? *Cell* 130, 395-398
6. de Godoy, L. M. et al. (2008) Comprehensive mass-spectrometry-based proteome quantification of haploid versus diploid yeast. *Nature* 455, 1251-1254
7. Witze, E. S., Old, W. M., Resing, K. A., and Ahn, N. G. (2007) Mapping protein post-translational modifications with mass spectrometry. *Nat. Methods* 4, 798-806
8. Macek, B., Mann, M., and Olsen, J. V. (2009) Global and site-specific quantitative phosphoproteomics: principles and applications. *Annu. Rev. Pharmacol. Toxicol.* 49, 199-221
9. Olsen, J. V. et al. (2006) Global, in vivo, and site-specific phosphorylation dynamics in signaling networks. *Cell* 127, 635-648
10. Golebiowski, F. et al. (2009) System-wide changes to SUMO modifications in response to heat shock. *Sci. Signal.* 2, ra24
11. Mayor, T., Graumann, J., Bryan, J., MacCoss, M. J., and Deshaies, R. J. (2007) Quantitative profiling of ubiquitylated proteins reveals proteasome substrates and the substrate repertoire influenced by the Rpn10 receptor pathway. *Mol. Cell Proteomics.* 6, 1885-1895
12. Peng, J. et al. (2003) A proteomics approach to understanding protein ubiquitination. *Nat. Biotechnol.* 21, 921-926
13. Schimmel, J. et al. (2008) The ubiquitin-proteasome system is a key component of the SUMO-2/3 cycle. *Mol. Cell Proteomics* 7, 2107-2122
14. Vertegaal, A. C. et al. (2004) A proteomic study of SUMO-2 target proteins. *J. Biol. Chem.* 279, 33791-33798
15. Vertegaal, A. C. et al. (2006) Distinct and overlapping sets of SUMO-1 and SUMO-2 target proteins revealed by quantitative proteomics. *Mol. Cell Proteomics* 5, 2298-2310
16. Wilson, V. G., and Heaton, P. R. (2008) Ubiquitin proteolytic system: focus on SUMO. *Expert. Rev. Proteomics* 5, 121-135
17. Pedrioli, P. G. et al. (2006) Automated identification of SUMOylation sites using mass spectrometry and SUMmOn pattern recognition software. *Nat. Methods* 3, 533-539
18. Matic, I. et al. (2008) In vivo identification of human small ubiquitin-like modifier polymerization sites by high accuracy mass spectrometry and an in vitro to in vivo strategy. *Mol. Cell Proteomics* 7, 132-144
19. Hsiao, H. H., Meulmeester, E., Frank, B. T., Melchior, F., and Urlaub, H. (2009) "ChopNSpice," a mass spectrometric approach that allows identification of endogenous small ubiquitin-like modifier-conjugated peptides. *Mol. Cell Proteomics* 8, 2664-2675
20. Makhnevych, T. et al. (2009) Global map of SUMO function revealed by protein-protein interaction and genetic networks. *Mol. Cell* 33, 124-135
21. Jeram, S. M., Srikumar, T., Pedrioli, P. G., and Raught, B. (2009) Using mass spectrometry to identify ubiquitin and ubiquitin-like protein conjugation sites. *Proteomics.* 9,

922-934

22. Knuesel, M., Cheung, H. T., Hamady, M., Barthel, K. K., and Liu, X. (2005) A method of mapping protein sumoylation sites by mass spectrometry using a modified small ubiquitin-like modifier 1 (SUMO-1) and a computational program. *Mol. Cell Proteomics* 4, 1626-1636
23. Wohlschlegel, J. A., Johnson, E. S., Reed, S. I., and Yates, J. R., III. (2006) Improved identification of SUMO attachment sites using C-terminal SUMO mutants and tailored protease digestion strategies. *J. Proteome. Res.* 5, 761-770
24. Blomster, H. A. et al. (2010) In vivo identification of sumoylation sites by a signature tag and cysteine-targeted affinity purification. *J. Biol. Chem.* 285, 19324-19329
25. Olsen, J. V. et al. (2007) Higher-energy C-trap dissociation for peptide modification analysis. *Nat. Methods* 4, 709-712
26. Olsen, J. V. et al. (2009) A dual pressure linear ion trap Orbitrap instrument with very high sequencing speed. *Mol. Cell Proteomics* 8, 2759-2769
27. Denison, C. et al. (2005) A proteomic strategy for gaining insights into protein sumoylation in yeast. *Mol. Cell Proteomics* 4, 246-254
28. Ikeda, F., and Dikic, I. (2008) Atypical ubiquitin chains: new molecular signals. 'Protein Modifications: Beyond the Usual Suspects' review series. *EMBO Rep.* 9, 536-542
29. Gnad, F. et al. (2007) PHOSIDA (phosphorylation site database): management, structural and evolutionary investigation, and prediction of phosphosites. *Genome Biol.* 8, R250
30. Choudhary, C. et al. (2009) Lysine acetylation targets protein complexes and co-regulates major cellular functions. *Science* 325, 834-840
31. Meulmeester, E., Kunze, M., Hsiao, H. H., Urlaub, H., and Melchior, F. (2008) Mechanism and consequences for paralog-specific sumoylation of ubiquitin-specific protease 25. *Mol. Cell* 30, 610-619
32. Zhuang, M. et al. (2009) Structures of SPOP-substrate complexes: insights into molecular architectures of BTB-Cul3 ubiquitin ligases. *Mol. Cell* 36, 39-50
33. Roukens, M. G. et al. (2008) Identification of a new site of sumoylation on Tel (ETV6) uncovers a PIAS-dependent mode of regulating Tel function. *Mol. Cell Biol.* 28, 2342-2357
34. Ross, S., Best, J. L., Zon, L. I., and Gill, G. (2002) SUMO-1 modification represses Sp3 transcriptional activation and modulates its subnuclear localization. *Mol. Cell* 10, 831-842
35. Gill, G. (2005) Something about SUMO inhibits transcription. *Curr. Opin. Genet. Dev.* 15, 536-541
36. Geiss-Friedlander, R., and Melchior, F. (2007) Concepts in sumoylation: a decade on. *Nat. Rev. Mol. Cell Biol.* 8, 947-956
37. Tashiro, S. et al. (2004) Repression of PML nuclear body-associated transcription by oxidative stress-activated Bach2. *Mol. Cell Biol.* 24, 3473-3484
38. Soderberg, O. et al. (2008) Characterizing proteins and their interactions in cells and tissues using the in situ proximity ligation assay. *Methods* 45, 227-232
39. Soderberg, O. et al. (2006) Direct observation of individual endogenous protein complexes in situ by proximity ligation. *Nat. Methods* 3, 995-1000
40. Mahajan, R., Gerace, L., and Melchior, F. (1998) Molecular characterization of the SUMO-1 modification of RanGAP1 and its role in nuclear envelope association. *J. Cell Biol.* 140, 259-270

41. Matunis, M. J., Wu, J., and Blobel, G. (1998) SUMO-1 modification and its role in targeting the Ran GTPase-activating protein, RanGAP1, to the nuclear pore complex. *J. Cell Biol.* 140, 499-509
42. Daub, H. et al. (2008) Kinase-selective enrichment enables quantitative phosphoproteomics of the kinome across the cell cycle. *Mol. Cell* 31, 438-448
43. Olsen, J. V. et al. (2006) Global, in vivo, and site-specific phosphorylation dynamics in signaling networks. *Cell* 127, 635-648
44. Golebiowski, F. et al. (2009) System-wide changes to SUMO modifications in response to heat shock. *Sci. Signal.* 2, ra24
45. Hietakangas, V. et al. (2006) PDSM, a motif for phosphorylation-dependent SUMO modification. *Proc. Natl. Acad. Sci. U. S. A* 103, 45-50
46. Mohideen, F. et al. (2009) A molecular basis for phosphorylation-dependent SUMO conjugation by the E2 UBC9. *Nat. Struct. Mol. Biol.* 16, 945-952
47. Yang, S. H., Galanis, A., Witty, J., and Sharrocks, A. D. (2006) An extended consensus motif enhances the specificity of substrate modification by SUMO. *EMBO J.* 25, 5083-5093
48. Schimmel, J. et al. (2010) Positively charged amino acids flanking a sumoylation consensus tetramer on the 110kDa tri-snRNP component SART1 enhance sumoylation efficiency. *J. Proteomics* 73, 1523-1534
49. Bernier-Villamor, V., Sampson, D. A., Matunis, M. J., and Lima, C. D. (2002) Structural basis for E2-mediated SUMO conjugation revealed by a complex between ubiquitin-conjugating enzyme Ubc9 and RanGAP1. *Cell* 108, 345-356
50. Xu, L. et al. (2003) BTB proteins are substrate-specific adaptors in an SCF-like modular ubiquitin ligase containing CUL-3. *Nature* 425, 316-321
51. Shevchenko, A., Tomas, H., Havlis, J., Olsen, J. V., and Mann, M. (2006) In-gel digestion for mass spectrometric characterization of proteins and proteomes. *Nat. Protoc.* 1, 2856-2860
52. Rappsilber, J., Mann, M., and Ishihama, Y. (2007) Protocol for micro-purification, enrichment, pre-fractionation and storage of peptides for proteomics using StageTips. *Nat. Protoc.* 2, 1896-1906
53. Cox, J., and Mann, M. (2008) MaxQuant enables high peptide identification rates, individualized p.p.b.-range mass accuracies and proteome-wide protein quantification. *Nat. Biotechnol.* 26, 1367-1372
54. Cox, J. et al. (2009) A practical guide to the MaxQuant computational platform for SILAC-based quantitative proteomics. *Nat. Protoc.* 4, 698-705

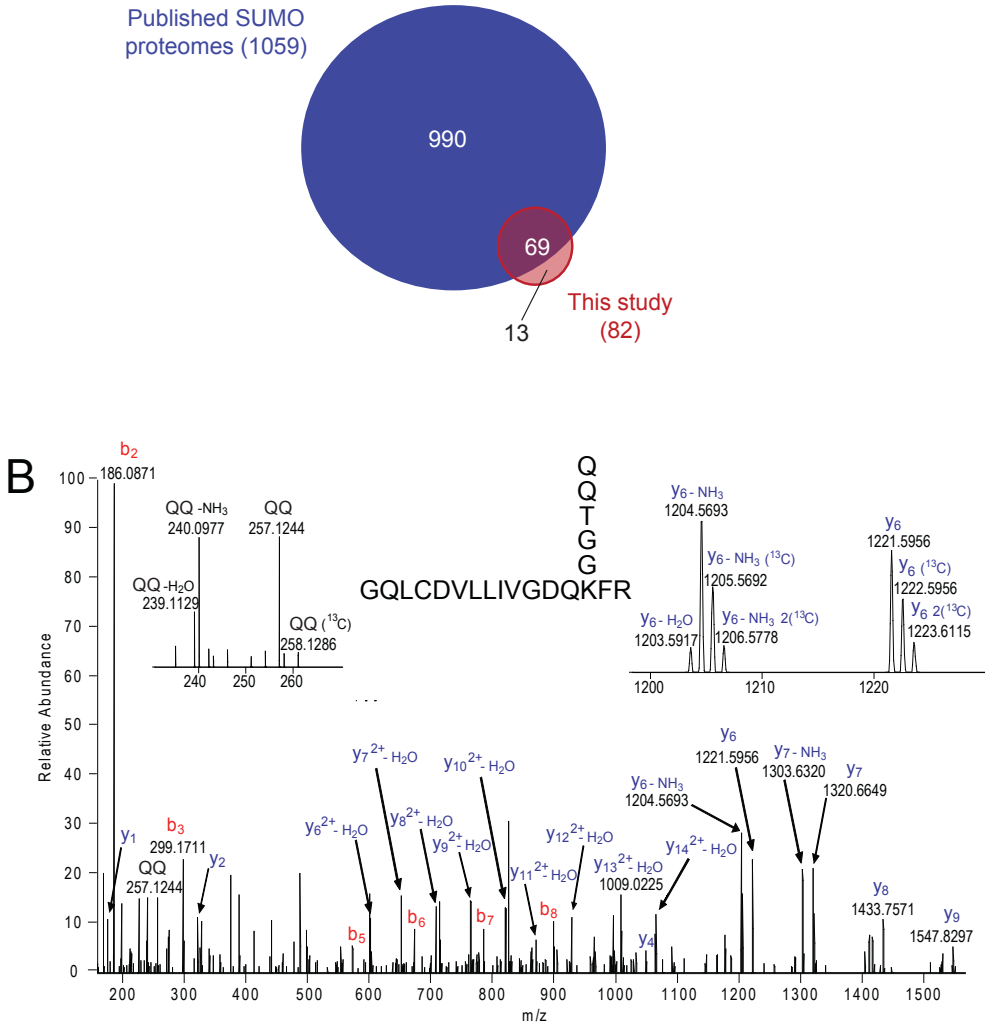

Figure S1.

A) Overlap between our study and previous SUMO proteomics projects. We have identified 103 SUMOylation sites in 82 SUMO target proteins including 69 SUMO target proteins that were previously identified as potential human SUMO target proteins [1-14]. Nine of the SUMO target proteins identified in this study have previously been identified as targets for Smt3; YFL039C, YKR092C, YKR008W, YJL148W, YEL026W, YLR335W, YDR390C, YOL006C and YNL088 (Denison et al., 2005; Panse et al., 2004; Wohlschlegel et al., 2004; Zhou et al., 2004).

B) HCD MS/MS spectrum showing the SUMOylation of ZNF295 via an inverted SUMOylation consensus site.

C and D) HCD MS/MS spectra showing the SUMOylation of type II cytoskeletal keratin 5.

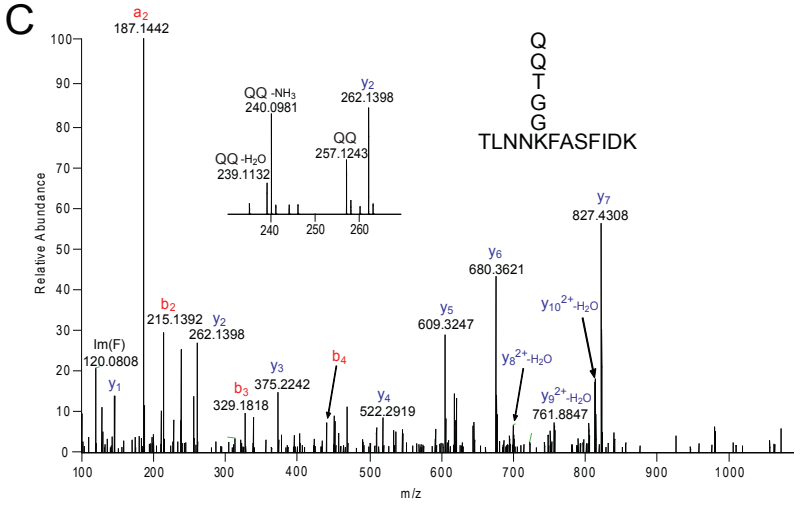

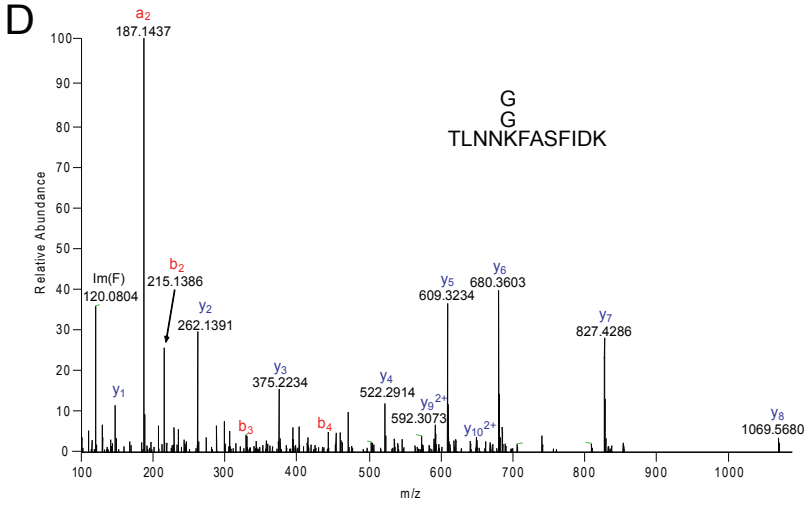

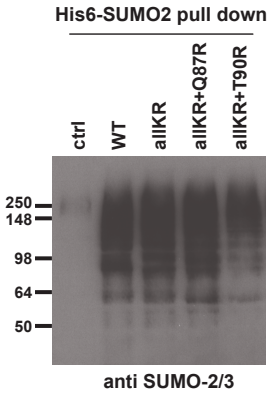

Figure S2.
Control immunoblot for Figure 2 probed with anti SUMO-2/3 antibody.

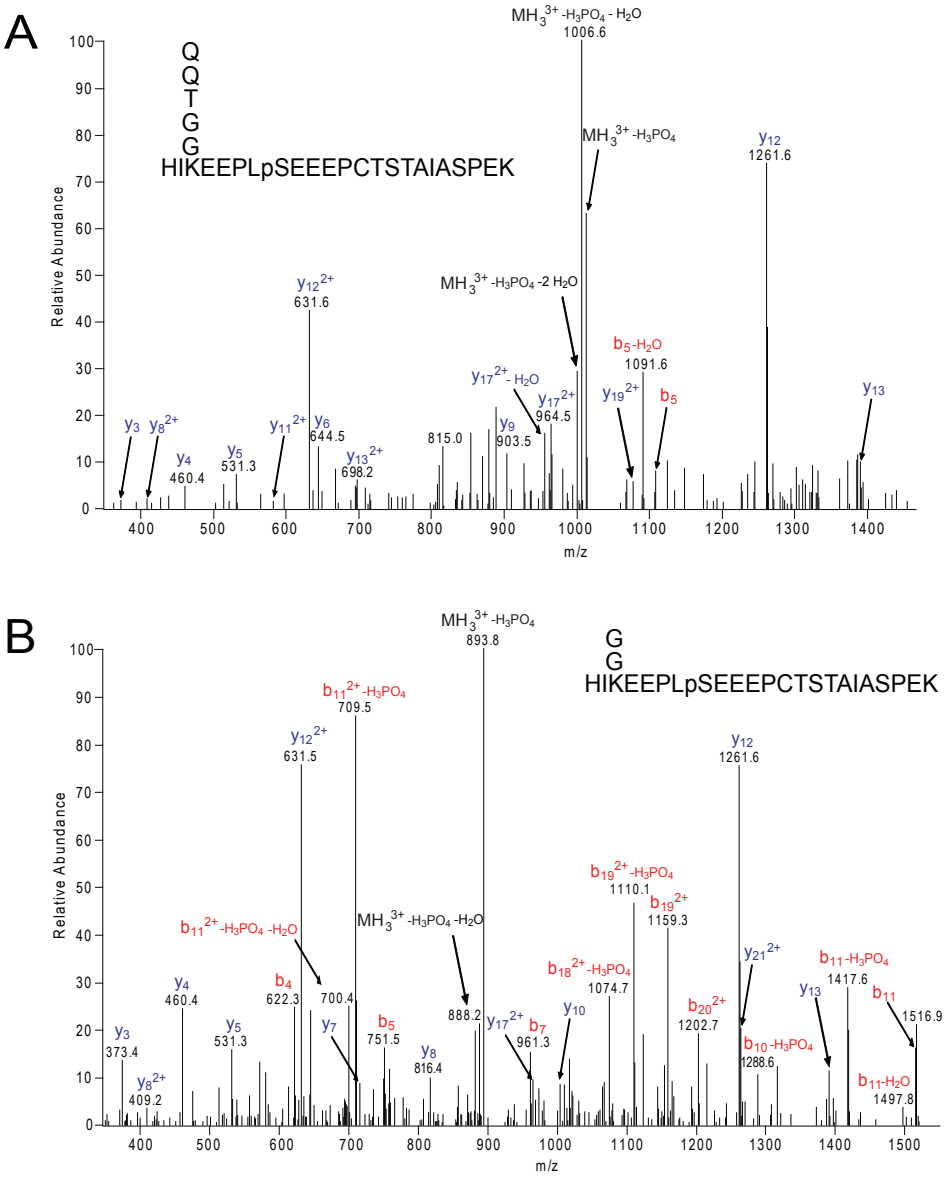

Figure S3.
A and B) CID MS/MS spectrum showing the phosphorylation-directed SUMOylation of NOP5/58.

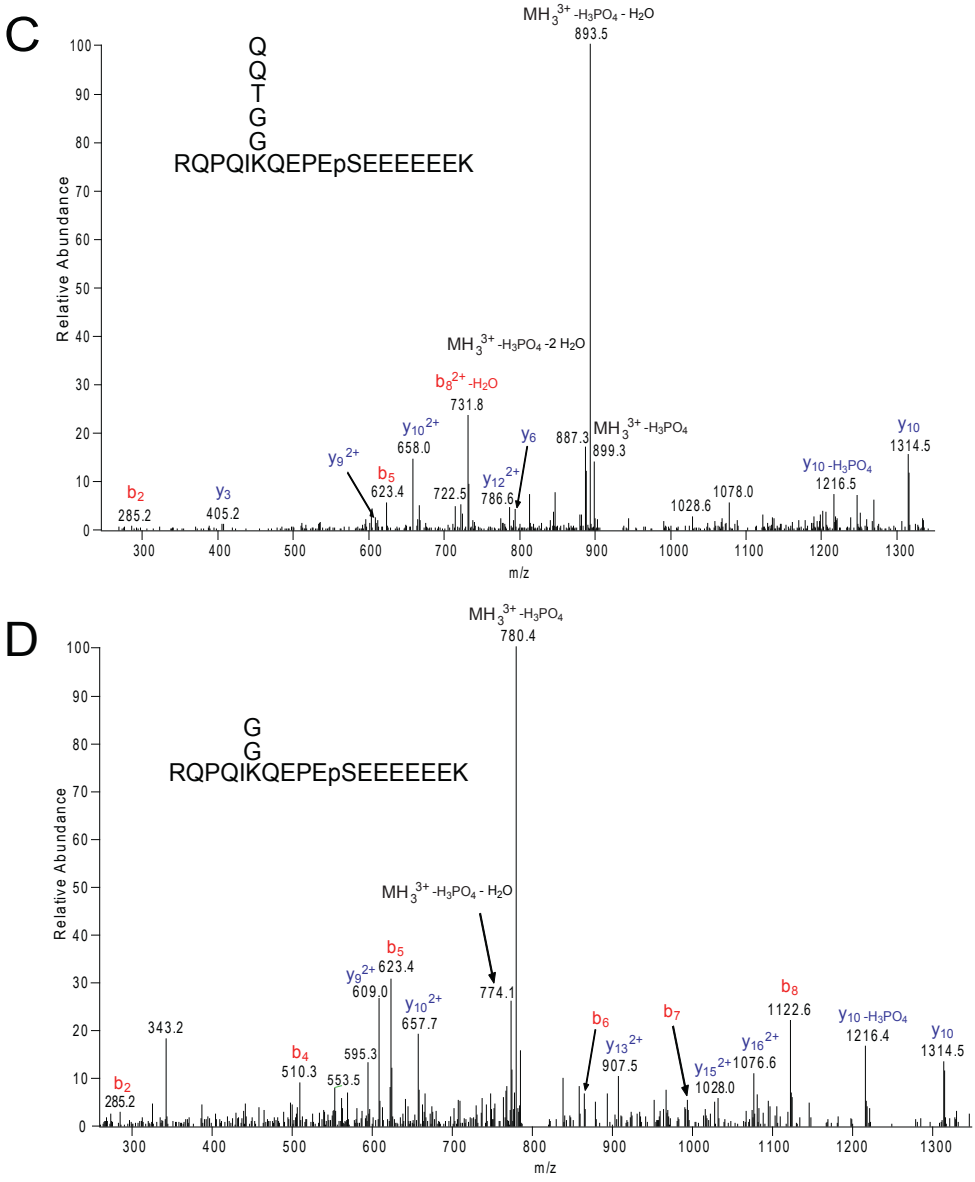

Figure S3.
C and D) CID MS/MS spectrum showing the phosphorylation-directed SUMOylation of RNA binding protein 25.

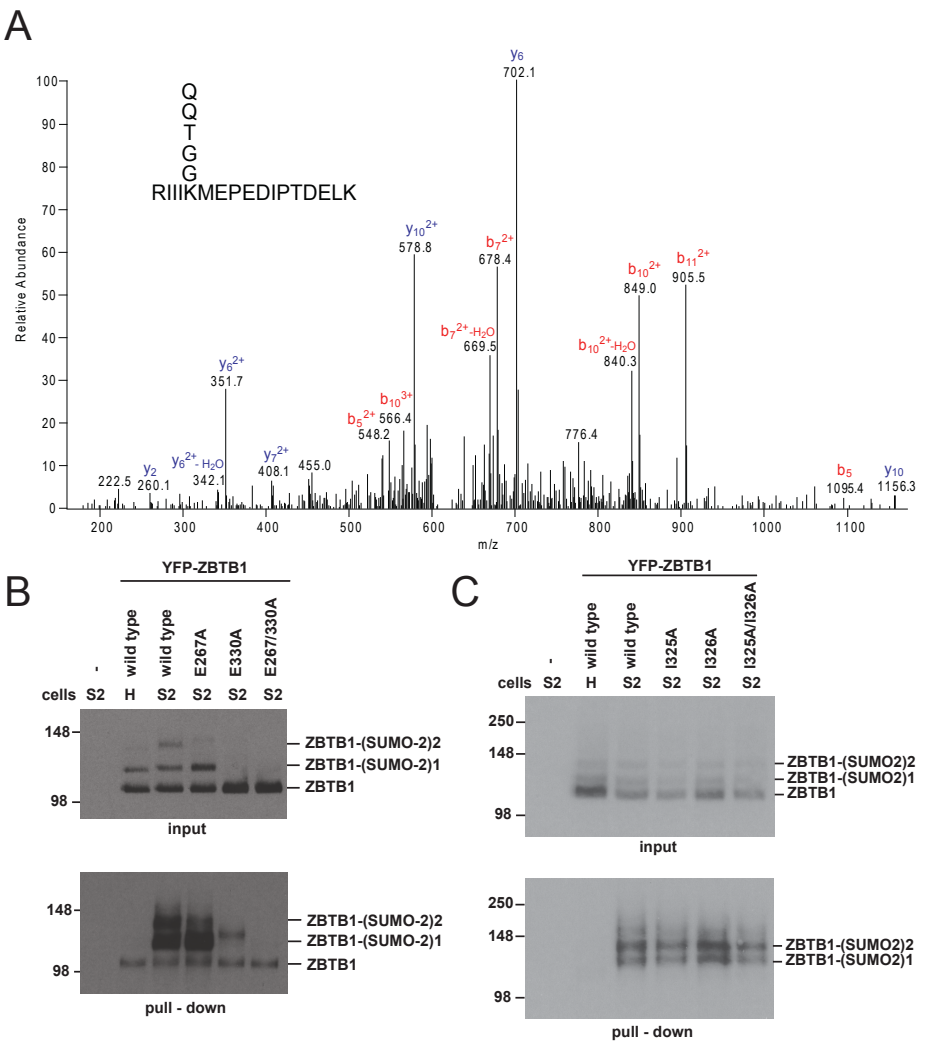

Figure S4.

A) CID MS/MS spectrum showing the SUMOylation of ZBTB1 via lysine 328.

B) SUMOylation analysis of YFP-ZBTB1 E267A, E330A single and double mutants. HeLa cells stably expressing His6-SUMO-2 (S2) and control HeLa (H) cells were transfected with expression constructs encoding YFP-ZBTB1 wild type, E267A, E330A single and double mutants. Cells were lysed 24 hours after transfection and His6-SUMO-2 conjugates were purified by IMAC. Total lysates (input) and purified fractions (pull down) were separated by SDS-PAGE, transferred to a membrane and probed using an antibody to detect YFP.

C) The ZBTB1 K328 SUMOylation site does not consist of an integrated SUMO Interaction Motif (SIM) and a SUMOylation site. SUMO-SIM interactions are depending on large hydrophobic residues in the SIM. We mutated the isoleucines in ZBTB1 on positions 325 and 326 to alanines and compared the SUMOylation efficiencies of the mutants to the wild-type protein. No reduction in SUMOylation was observed for the mutants, indicating that the K328 SUMOylation site in ZBTB1 does not consist of an integrated SUMO Interaction Motif (SIM) and a SUMOylation site.

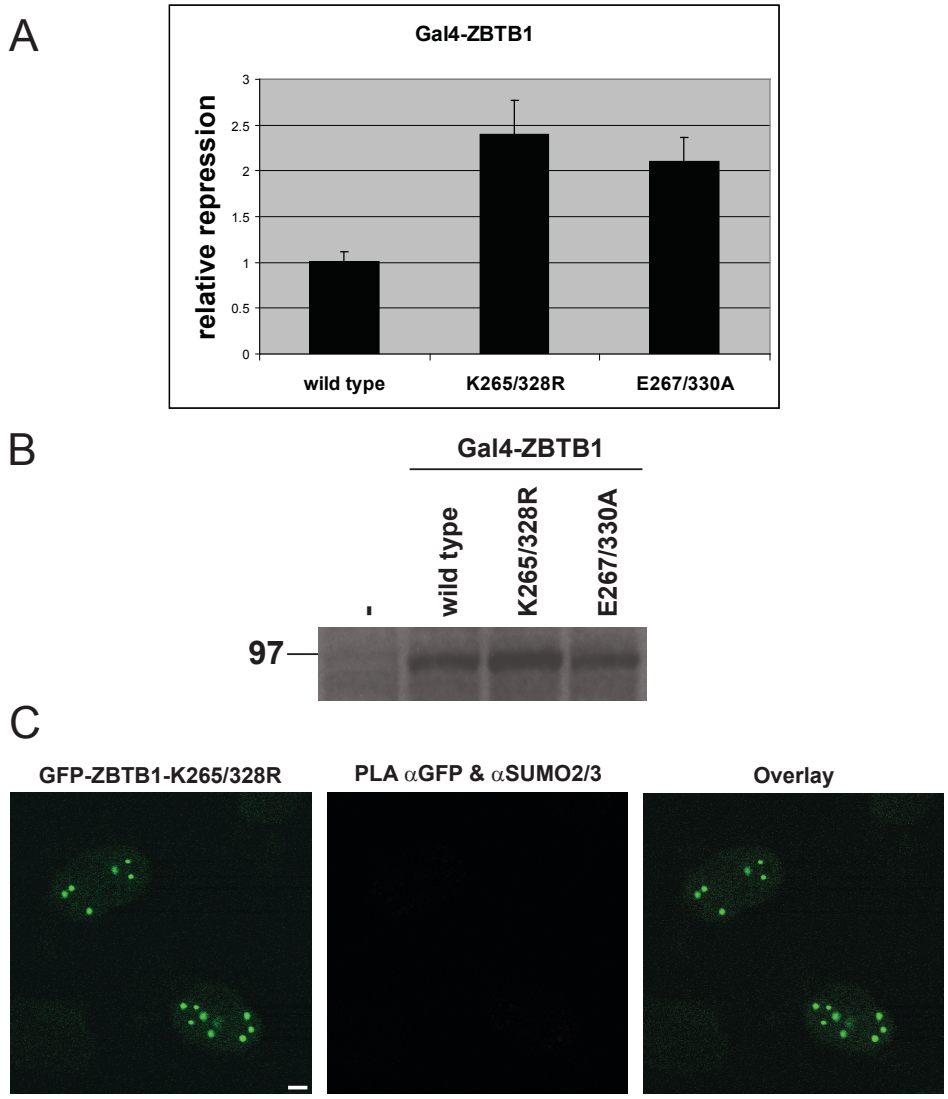

Figure S5.

A and B) GAL4-ZBTB1-E267A-E330A luciferase activity and immunoblot. HeLa cells were grown on 24-well dishes and transfected with 500 ng of Gal4(DBD)-fusion expression plasmids and 500 ng of the reporter construct 5xGal4-Tk-Pgl3. Cells were lysed in reporter lysis buffer and luciferase activity was measured. (A) The transcriptional activities of Gal4-ZBTB1 wild type and SUMOylation mutants were determined. The error bars indicate one standard deviation from the average; results are representative of five independent experiments. (B) Transfection mixtures were split and one set of wells was lysed in LDS sample buffer to verify the expression levels of the Gal4-ZBTB1 proteins by immunoblotting using an antibody directed against Gal4.

C) GFP-ZBTB1-K265R-K328R PLA negative control. HeLa cells were transfected with an expression construct encoding GFP-ZBTB1-K265R-K328R, fixed and the PLA was performed using affinity purified peptide anti SUMO-2/3 antibodies and a monoclonal antibody directed against GFP. Secondary antibodies were labeled with specific oligonucleotides. Oligonucleotide hybridization, ligation, amplification and detection were performed.

Supplemental Experimental Procedures

Plasmids

Lysine-deficient SUMO-2 was previously described [11]. Lysine-deficient SUMO2-Q87R was generated by QuickChange site-directed mutagenesis (Stratagene) using oligonucleotides 5'-CATCGACGTGTTC-CGGCAGCAGACGGGAG-3' and 5'-CTCCCGTCTGCTGCCGGAACACGTCGATG-3' and lysine-deficient SUMO2-T90R was generated using oligonucleotides 5'-GTGTTCCAGCAGCAGAGGGGAGGTTAGGAAT-TCTG-3' and 5'-CAGAATTCCTAACCTCCCCTCTGCTGCTGGAACAC-3'.

The cDNA encoding the ZBTB1 protein was obtained from the Mammalian Gene Collection (MGC code 60335; Image ID 6141266; supplied by MRC geneservice, Cambridge, UK) and amplified by a two-step PCR reaction using the following primers: 5'-AAAAAGCAGGCTATATGGCAAAGCCCAGCCAC-3' and 5'-AGAAAGCTGGGTCTCAGGTTCTTTTCAAATGC-3' for the first reaction and 5'-GGGGACAAGTTTG-TACAAAAAAGCAGGCT-3' and 5'-GGGGACCACTTTGTACAAGAAAGCTGGGT-3' for the second reaction. The forward primer for the mutant lacking the BTB domain was 5'-AAAAAGCAGGCTATATGCAGGATG-CAGATTGTTC-3'. The cDNA was inserted into pDON207 employing standard Gateway technology (Invitrogen) and subsequently transferred to multiple different destination vectors to generate a T7-ZBTB1 expression construct and EYFP-, ECFP- EGFP- and GAL4(DBD)-tagged ZBTB1 expression plasmids. The fusions were made to the N-terminus of ZBTB1. EYFP-, ECFP- and EGFP-destination vectors were constructed by Dr. M. Posch (Wellcome Trust Biocentre, Dundee, UK). The Gal4(DBD)-destination vector was obtained by ligation of the Gateway cassette reading frame B (Invitrogen) into the *Eco*RI digested pCG4 plasmid [15], which was a kind gift of Dr. N.D. Perkins (Wellcome Trust Biocentre, Dundee, UK). T7-ZBTB1 was constructed using destination vector pDEST14 (Invitrogen).

To generate ZBTB1 SUMOylation site mutants, the consensus SUMOylation sites, lysine 265 and lysine 328, were mutated to arginine residues by QuickChange site-directed mutagenesis (Stratagene) using oligonucleotides 5'-GACAGTAACATCAGAGCTGAATTTGGTG-3' and 5'-CACCAAAT-TCAGCTCTGATGTTACTGTC-3' for the K265R mutation, 5'-GGATTATTATTAGGATGGAGCCAGAAG-3' and 5'-CTTCTGGCTCCATCCTAATAATAATCC-3' for the K328R mutation, 5'-GACAGTAACATCAAAGCTG-CATTTGGTGAAAAAG-3 and 5'-CTTTTTCACCAAATGCAGCTTTGATGTTACTGTC-3' for the E267A mutation and 5'-GGATTATTATTAAGATGGCTCCAGAAGATATTCCTAC-3' and 5'-GTAGGAATATCTTCTGGAGCCATCT-TAATAATAATCC-3' for the E330A mutation.

To generate mutations in the hydrophobic cluster preceding the SUMOylated lysine K328, we replaced isoleucines on positions 325 and 326 for the corresponding amino acids preceding the SUMOylated lysine 265, serine and asparagine respectively using oligonucleotides 5'-CTGA-GAGAAAAGGAGTATTATTAAGATGGAG-3' and 5'-CTCCATCTTAATAATACTCCTTTTCCTCTCAG-3' for the I325S mutation and oligonucleotides 5'-GAGAGGAAAAGGATTAATATTAAGATGGAGCC-3' and 5'-GGCTC-CATCTTAATATTAATCCTTTTCCTCTC-3' for the I326N mutation. The I325A mutation was generated using oligonucleotides 5'-CTGAGAGGAAAAGGGCTATTATTAAGATGGAG-3' and 5'-CTCCATCTTAATAATAGC-CCTTTTCCTCTCAG-3'. The I326A mutation was generated using oligonucleotides 5'-GAGAGGAAAAG-GATTGCTATTAAGATGGAGCC-3' and 5'-GGCTCCATCTTAATAGCAATCCTTTTCCTCTC-3'.

The BTB domain (aa1-141) of ZBTB1 was amplified using oligonucleotides 5'-ACAACGGATC-CATGGCAAAGCCCAGCCAC-3' and 5'-GCCGCGGAATTCTTACCCAAATATCATTTTGCTG-3' and inserted into pGEX-2T.

Phosphorylation site mutants in NOP5/58-EGFP (a kind gift from Dr. Westman, Dundee, U.K.) were generated by site directed mutagenesis. The S502A mutant was generated using oligonucleotides 5'-GGAAGAACCACTTGCTGAGGAAGAACCATG-3' and 5'-CATGGTTCTTCCTCAGCAAGTGGTTCTTCC-3'. The S502D mutant was generated using oligonucleotides 5'-GGAAGAACCACTTGATGAGGAAGAAC-CATG-3' and 5'-CATGGTTCTTCCTCATCAAGTGGTTCTTCC-3'.

The HA-RanGAP1 expression construct was a kind gift from Dr. Melchior (Heidelberg, Germany). The Δ523_524 mutant was generated using oligonucleotides 5'-GGCTCCTCGTGCACATGCT-CAAGAGTGAAGACAAG-3' and 5'-CTTGTCTTCACTCTTGAGCATGTGCACGAGGAGCC-3'. The G523H-L524H mutant was generated using oligonucleotides 5'-GGCTCCTCGTGCACATGCATCACCTCAAGAGTGAAG-ACAAGG-3' and 5'-CCTTGTCTTCACTCTTGAGGTGATGCATGTGCACGAGGAGCC-3'. The G523N_L524N

mutant was generated using oligonucleotides 5'-CAGGCTCCTCGTGCACATGAATAACCTCAAGAGTGAAG-ACAAGG-3' and 5'-CCTTGTCTTCACTCTTGAGGTTATTCATGTGCACGAGGAGCCTG-3'.

pCMX-SMRTe [16, 17] was a kind gift of Dr. E.J. Park and Dr. J.D. Chen (University of Massachusetts Medical School, Worcester, MA). The SMRT cDNA was amplified by PCR using pCMX-hSMRTe as template and oligonucleotides 5'-GGGGACAAGTTTGTACAAAAAAGCAGGCTCCATGTCGGGCTCCA-CACAGCCTGT-3' and 5'-GGGGACCACTTTGTACAAGAAAGCTGGGTGTCACTCGCTGTCGGAGAGTGTCT-CGTA-3'. The amplified fragment was subsequently inserted into pDON207, and the EYFP-SMRT expression construct was obtained using standard Gateway technology. Constructs were verified by sequencing.

***In vivo* SUMO conjugation assays**

HeLa cells stably expressing His6-SUMO-2 and control HeLa cells were grown on 15cm culture dishes and transfected. Cells were isolated by trypsinization 24 hours after transfection, washed twice with ice-cold PBS and lysed in 1 ml lysis buffer containing 8 M urea, 100 mM Na2HPO4/NaH2PO4 and 10 mM Tris/HCl pH 7.0 at room temperature. After removal of DNA clumps, samples were sonicated 4x 5 secs on ice. Imidazole (5mM) was added where indicated and His6-SUMO-2 conjugates were purified on 50 µl Co^{2+} TALON beads (BD Biosciences) at room temperature. After washing the beads four times with 1 ml urea lysis buffer, SUMO-2 conjugates were eluted from the beads in 60 µl urea lysis buffer containing 200 mM imidazole. Alternatively, cells were solubilized in lysis buffer (6 M Guanidinium-HCl, 100 mM Na2HPO4/NaH2PO4, 10 mM Tris/HCl, pH 8.0, 20 mM Imidazole, 10 mM β mercapto-ethanol) and sonicated to reduce the viscosity. His6-SUMO conjugates were enriched on Ni-NTA Agarose beads (Qiagen) and washed using wash buffers A-D. (Buffer A: 6 M Guanidinium-HCl, 100 mM NaH2PO4 / Na2HPO4, 10 mM Tris/HCl pH 8.0 and 0.2% Triton-X-100. Buffer B: 8 M Urea, 100 mM NaH2PO4 / Na2HPO4, 10 mM Tris/HCl pH 8.0 and 0.2% Triton-X-100. Buffer C: 8 M Urea, 100 mM NaH2PO4 / Na2HPO4, 10 mM Tris/HCl pH 6.3 and 0.2% Triton-X-100. Buffer D: 8 M Urea, 100 mM NaH2PO4 / Na2HPO4, 10 mM Tris/HCl pH 6.3 and 0.1% Triton-X-100). These wash buffers also contained 10 mM β mercapto-ethanol. Samples were eluted in 6.4 M Urea, 80 mM NaH2PO4/Na2HPO4, 8 mM Tris/HCl pH 7.0, 200 mM imidazole.

Electrophoresis and immunoblotting

Protein samples were size fractionated on Novex 4-12% Bis-Tris gradient gels using MOPS running buffer (Invitrogen) or on regular SDS-PAGE gels with a tris-glycine buffer. Note that these different methods cause slight differences in the running behavior of proteins (Invitrogen). Size fractionated proteins were subsequently transferred onto Hybond-C extra membranes (Amersham Biosciences) using a submarine system (Invitrogen). Blots were stained for total protein using Ponceau S (Sigma). After blocking with PBS containing 0.1% Tween-20 and 5% milk powder, the membranes were incubated with primary antibodies as indicated.

Electrophoresis, Coomassie Staining and In-gel digestion

The purified His6-SUMO-2 conjugates were separated by SDS-PAGE using Novex 4-12% gradient gels and MES SDS running buffer (Invitrogen), followed by staining with Colloidal Blue Kit (Invitrogen). Bands in the molecular range of 15-38 kDa were excised from the gel, cut into 2-mm^3 cubes and in-gel digested with trypsin (Promega) essentially as described [18]. The reduction and alkylation steps were performed before Lys-C digestion and therefore skipped during trypsin in-gel digestion. The peptides extracted from the gel after digestion were cleaned, desalted, concentrated and enriched on C_{18} reverse phase StageTips [19]. In-solution digested samples were analyzed on an LTQ-Orbitrap XL mass spectrometer whereas the analysis of in-gel digested samples was performed on an LTQ-Orbitrap Velos instrument [20].

Liquid Chromatography-Mass spectrometry

Mass spectrometric analysis was performed by nanoscale LC-MS/MS using LTQ-Orbitrap XL and LTQ-Orbitrap Velos instruments (Thermo Fisher Scientific, Germany) coupled to an EASY-nLC system

(Proxeon Biosystems, Denmark) via a Proxeon nanoelectrospray interface. Peptides eluted from StageTips were separated on a 75 µm inner diameter reverse phase C_{18} column packed in-house with 3 µm C18 beads (Dr. Maisch, Germany) with a 140 or 240 min gradient.

Data were acquired in data-dependent mode. In the case of the LTQ-Orbitrap XL, full scan spectra were acquired in the 300-1600 m/z range (*R* = 60,000 and target value of 1,000,000); 400-1000 m/z range was used in the 'single range' method; 'multiple ranges' experiments used mass regions m/z 300-500, m/z 450-650, m/z 600-900, m/z 850-1,250, m/z 1,200-1,800. Injection waveforms option was enabled in all survey scans to eject all ions outside of the specified mass range. For 'full range' and 'single range' orbitrap measurements the "lock mass" option was used to improve the mass accuracy of precursor ions [21]. The ten most intense ions were fragmented by collision-induced dissociation (CID) with normalized collision energy of 35% and recorded in the linear ion trap (target value of 5,000) based on the survey scan and in parallel to the orbitrap detection of MS spectra. In the case of the LTQ-Orbitrap Velos, survey scan acquisition was performed in the orbitrap with a resolution of 30,000 at m/z 400. Ten most intense ions were fragmented by higher-energy collisional dissociation (HCD) with normalized collision energy of 40% and recorded in the orbitrap with a resolution of 7,500 at m/z 400 (target value of 50,000). The HCD experiments were performed in the 'full range' mode (300-1700 m/z: target value of 1,000,000) and 'multiple ranges' mode (mass ranges of 400-650 m/z, 600-900 m/z and 850-1300 m/z; target value of 500'000). Survey and HCD fragment spectra were acquired in profile mode, whereas the acquisition of CID MS/MS spectra was done in centroid mode.

Data Processing and Analysis

Raw MS data files were processed with the MaxQuant software (version 1.0.14.3)[22] as previously described [23]. Enzyme specificity was set to trypsin, allowing for cleavage N-terminal to proline residues and up to four missed cleavages. Cysteine carbamidomethylation was considered as a fixed modification, and methionine oxidation, protein N-acetylation and phosphorylation on serine, threonine and tyrosine residues were set as variable modifications in all experiments. In addition, mass addition of 114.0429 (GG signature tag derived from SUMO2-T90R) on lysine for the T90R experiment, and mass addition of 471.2078 (QQTGG signature tag remnant of SUMO2-Q87R) on lysine for the Q87R experiment, were considered as variable modifications. MS/MS peak list generated by MaxQuant were searched by the Mascot database search engine (Matrix Science, London, UK, version 2.1.04) against the human International Protein Index (IPI) database (version 3.37)(Kersey et al., 2004). The initial maximum allowed mass deviation was set to 7 ppm for peptide masses, 0.5 Da for low resolution CID fragment ions and 0.02 Da for high resolution HCD fragment ions.

Manual validation of Peptide Identifications

The best MS/MS spectra of all identified SUMOylated peptides were manually validated using the Viewer module of MaxQuant and Xcalibur Qual browser instruments (Thermo Fisher Scientific, Germany). The peptide matches were filtered by the following criteria: (i) maximum mass deviation smaller than 5 ppm; (ii) only peptides containing an internal SUMOylated lysine were accepted; (iii) reasonable coverage of b- and/or y- ions series; (iv) peptides containing prolines were required to show pronounced cleavage amino-terminal to the proline residue; (v) preferential cleavage C-terminally from aspartate and glutamate; (vi) presence of a_2/b_2 pairs. Additionally, Q87R HCD spectra were required to show QQTGG signature fragment ions in the low mass region: m/z 257.125 (QQ), m/z 240.097 (QQ with loss of ammonia) and m/z 239.114 (QQ with loss of water).

***In vitro* expression of proteins**

In vitro transcription/translation of proteins was performed using 1 µg of plasmid DNA (T7-ZBTB1) and a wheat germ-coupled transcription/translation system in 25 µl reaction volumes according to the instructions provided by the manufacturer (Promega). [35S]Methionine (17.5 µCi per labeling) (Amersham Biosciences) was used in the reactions to generate radiolabeled proteins.

In vitro SUMO conjugation assays

In vitro SUMO conjugation assays were performed in 10 µl volumes containing 120 ng SAE1/2, 500 ng SUMO-2, 50 mM Tris/HCl pH 7.5, 5 mM MgCl2, 2 mM ATP, 10 mM creatine phosphate, 3.5 U/ml creatine kinase, 0.6 U/ml inorganic pyrophosphatase, protease inhibitors and Ubc9 as indicated. SUMOylation was carried out using 1 µl of the *in vitro* transcribed and translated [35S] labeled ZBTB1 or 30 µM peptide. Reactions were incubated for 3 hours at 37°C. After termination of the reaction with LDS sample buffer (Invitrogen), reaction products were fractionated by SDS-PAGE using Novex 4-12% Bis-Tris gradient gels and MOPS running buffer (Invitrogen). Dried gels were exposed to X-Omat AR (XAR) autoradiography films (Kodak) to detect radiolabeled proteins.

Luciferase assays

HeLa cells were grown on 24-well tissue culture plates and transfected with 500 ng of Gal4-DBD or Gal4(DBD)-fusion expression plasmids and 500 ng of the reporter construct 5xGal4-Tk-Pgl3 [24]. 24 hours after transfection, cells were washed with ice-cold PBS and lysed in 100 µl reporter lysis buffer (Promega). As a control, the luciferase activity of the known transcriptional repressor thyroid hormone receptor (TR) was determined [25]. Luciferase activity relative to Gal4-DBD was depicted. Equal expression of Gal4(DBD)-fusion plasmids was verified by immunoblotting. Transfection mixtures were split over two wells. Samples for immunoblotting were prepared in LDS sample buffer (Invitrogen).

Proximity Ligation Assay

Proximity Ligation was performed as previously described [26, 27]. Cells were fixed for 15 minutes with 3.7% paraformaldehyde in PBS at 37°C and permeabilized for 15 minutes at room temperature with 0.1% Triton X-100 in TBS. After washing, cells were blocked for 10 minutes using 0.5% milk powder in TBST. Antibody incubations using monoclonal anti GFP antibody (Roche) and affinity purified rabbit anti SUMO-2/3 antibody (Eurogentec) were carried out overnight in blocking solution at room temperature. Subsequent steps were carried out at 37°C. Secondary antibodies were incubated for 1 hour. Hybridization was performed for 30 minutes in a humid chamber. This chamber was also used for ligation for 30 minutes, for amplification for 90 minutes and for detection for 30 minutes. Dot-like structures are an intrinsic characteristic of PLA signals and do not necessarily represent nuclear bodies.

Supplemental Reference List

1. Blomster, H. A. et al. (2009) Novel proteomics strategy brings insight into the prevalence of SUMO-2 target sites. *Mol. Cell Proteomics* 8, 1382-1390
2. Ganesan, A. K. et al. (2007) Broad spectrum identification of SUMO substrates in melanoma cells. *Proteomics* 7, 2216-2221
3. Gocke, C. B., Yu, H., and Kang, J. (2005) Systematic identification and analysis of mammalian small ubiquitin-like modifier substrates. *J. Biol. Chem.* 280, 5004-5012
4. Golebiowski, F. et al. (2009) System-wide changes to SUMO modifications in response to heat shock. *Sci. Signal.* 2, ra24
5. Li, T. et al. (2004) Sumoylation of heterogeneous nuclear ribonucleoproteins, zinc finger proteins, and nuclear pore complex proteins: a proteomic analysis. *Proc. Natl. Acad. Sci. U. S. A* 101, 8551-8556
6. Li, T. et al. (2006) A general approach for investigating enzymatic pathways and substrates for ubiquitin-like modifiers. *Arch. Biochem. Biophys.* 453, 70-74
7. Manza, L. L. et al. (2004) Global shifts in protein sumoylation in response to electrophile and oxidative stress. *Chem. Res. Toxicol.* 17, 1706-1715
8. Matafora, V., D'Amato, A., Mori, S., Blasi, F., and Bachi, A. (2009) Proteomics analysis of nucleolar SUMO-1 target proteins upon proteasome inhibition. *Mol. Cell Proteomics* 8, 2243-2255

9. Pungaliya, P. et al. (2007) TOPORS functions as a SUMO-1 E3 ligase for chromatin-modifying proteins. *J. Proteome. Res.* 6, 3918-3923
10. Rosas-Acosta, G., Russell, W. K., Deyrieux, A., Russell, D. H., and Wilson, V. G. (2005) A universal strategy for proteomic studies of SUMO and other ubiquitin-like modifiers. *Mol. Cell Proteomics* 4, 56-72
11. Schimmel, J. et al. (2008) The ubiquitin-proteasome system is a key component of the SUMO-2/3 cycle. *Mol. Cell Proteomics* 7, 2107-2122
12. Vertegaal, A. C. et al. (2004) A proteomic study of SUMO-2 target proteins. *J. Biol. Chem.* 279, 33791-33798
13. Vertegaal, A. C. et al. (2006) Distinct and overlapping sets of SUMO-1 and SUMO-2 target proteins revealed by quantitative proteomics. *Mol. Cell Proteomics* 5, 2298-2310
14. Zhao, Y., Kwon, S. W., Anselmo, A., Kaur, K., and White, M. A. (2004) Broad spectrum identification of cellular small ubiquitin-related modifier (SUMO) substrate proteins. *J. Biol. Chem.* 279, 20999-21002
15. Chapman, N. R., and Perkins, N. D. (2000) Inhibition of the RelA(p65) NF-kappaB subunit by Egr-1. *J. Biol. Chem.* 275, 4719-4725
16. Park, E. J. et al. (1999) SMRTe, a silencing mediator for retinoid and thyroid hormone receptors-extended isoform that is more related to the nuclear receptor corepressor. *Proc. Natl. Acad. Sci. U. S. A* 96, 3519-3524
17. Wu, X., Li, H., Park, E. J., and Chen, J. D. (2001) SMRTE inhibits MEF2C transcriptional activation by targeting HDAC4 and 5 to nuclear domains. *J. Biol. Chem.* 276, 24177-24185
18. Shevchenko, A., Tomas, H., Havlis, J., Olsen, J. V., and Mann, M. (2006) In-gel digestion for mass spectrometric characterization of proteins and proteomes. *Nat. Protoc.* 1, 2856-2860
19. Rappsilber, J., Mann, M., and Ishihama, Y. (2007) Protocol for micro-purification, enrichment, pre-fractionation and storage of peptides for proteomics using StageTips. *Nat. Protoc.* 2, 1896-1906
20. Olsen, J. V. et al. (2009) A dual pressure linear ion trap Orbitrap instrument with very high sequencing speed. *Mol. Cell Proteomics* 8, 2759-2769
21. Olsen, J. V. et al. (2005) Parts per million mass accuracy on an Orbitrap mass spectrometer via lock mass injection into a C-trap. *Mol. Cell Proteomics* 4, 2010-2021
22. Cox, J., and Mann, M. (2008) MaxQuant enables high peptide identification rates, individualized p.p.b.-range mass accuracies and proteome-wide protein quantification. *Nat. Biotechnol.* 26, 1367-1372
23. Cox, J. et al. (2009) A practical guide to the MaxQuant computational platform for SILAC-based quantitative proteomics. *Nat. Protoc.* 4, 698-705
24. Kalkhoven, E., Teunissen, H., Houweling, A., Verrijzer, C. P., and Zantema, A. (2002) The PHD type zinc finger is an integral part of the CBP acetyltransferase domain. *Mol. Cell Biol.* 22, 1961-1970
25. Tone, Y., Collingwood, T. N., Adams, M., and Chatterjee, V. K. (1994) Functional analysis of a transactivation domain in the thyroid hormone beta receptor. *J. Biol. Chem.* 269, 31157-31161
26. Soderberg, O. et al. (2008) Characterizing proteins and their interactions in cells and tissues using the in situ proximity ligation assay. *Methods* 45, 227-232
27. Soderberg, O. et al. (2006) Direct observation of individual endogenous protein complexes in situ by proximity ligation. *Nat. Methods* 3, 995-1000